# Continental shelf glaciations off Northeast Greenland since the late Miocene

Frank W. Jakobsen[1,2], Monica Winsborrow[1], Tove Nielsen[3], Jan Sverre Laberg[4], Andreia Plaza-Faverola[1], Christoph Böttner[5,6], Adrián López-Quirós[7], Sverre Planke[8,9], Benjamin Bellwald[8,10]

1. iC3 – Centre for ice, Cryosphere, Carbon and Climate, Department of Geosciences, UiT The Arctic University of Norway, Tromsø, Norway.
2. Geological Survey of Norway, Trondheim, Norway.
3. The National Geological Survey of Denmark and Greenland (GEUS), Copenhagen, Denmark.
4. Department of Geosciences, UiT The Arctic University of Norway, Tromsø, Norway.
5. Department of Geoscience, Aarhus University, Aarhus C, Denmark.
6. Department of Geological Sciences, Stockholm University, Stockholm, Sweden.
7. Department of Stratigraphy and Palaeontology, University of Granada, Granada, Spain.
8. Volcanic Basin Energy Research, Oslo, Norway.
9. Department of Geosciences, University of Oslo, Oslo, Norway.
10. The Norwegian Geotechnical Institute, Oslo, Norway.

*Correspondence to: Frank W. Jakobsen (Frank.Jakobsen@uit.no)*

**Abstract.** Amplified Arctic warming is triggering dramatic changes to the Greenland Ice Sheet (GrIS). Studying past warm periods can provide process insights valuable to predictions of future ice sheet response. Miocene (23.03 – 5.33 Ma) and Pliocene (5.33 – 2.58 Ma) global climatic records include periods of warmer than present temperatures thought to represent analogues to near-future scenarios. Despite this, the details of the long-term glacial history of the eastern and northeastern sectors of Greenland are still largely unresolved. Here, we use seismic reflection and borehole data to describe the late Cenozoic glacial architectural development of the Northeast Greenland continental margin and thereby reconstruct long-term ice sheet evolution. We identify three key unconformable seismic surfaces that define three mega units of predominantly glacial origin. Two of the surfaces are for the first time correlated across the entire outer Northeast Greenland margin and tied to both Ocean Drilling Program Sites 909 and 913. We show that the late Miocene onset of shelf progradation occurs around 6.4 Ma, marking the first recorded advance of grounded ice masses across the NE Greenland shelf, forming depocentres (trough mouth fans) beyond the palaeo-shelf edge. Subsequently during the late Miocene and early Pliocene, the GrIS expands multiple times across the shelf, extending the continental shelf seawards. Based on the development of more extensive and thicker depocentres along the entire outer shelf and upper slope, we suggest an intensification of shelf glaciations after ~4.1 Ma, possibly coinciding with the intensification of the Northern Hemisphere glaciations (3.6 – 2.7 Ma).

## 1 Introduction

Greenland currently hosts the largest ice sheet in the Northern Hemisphere, which if melted completely would raise global sea level by 7 m (Shepherd et al., 2020; and references therein). Over the Cenozoic, the thickness and extent of the Greenland Ice Sheet (GrIS) has varied, at times extending beyond the coastline and across the continental shelf (e.g., Funder et al., 2011; Knutz et al., 2019). The widest continental shelf in Greenland is in the northeast, and the inland ice sheet sector is currently drained by the Northeast Greenland Ice Stream (NEGIS; Fig. 1a), which drains 16% of the total area of the entire GrIS (Hvidberg et al., 2020). Despite the large size of the NE Greenland shelf and the importance of the NEGIS to present-day ice dynamics and stability in this ice sheet sector, little is known about the long-term glacial history of the area, including the timing and evolution of continental shelf glaciations. Such knowledge is needed to assess ice sheet-climate interactions beyond observational timescales and to reliably represent the GrIS in historical global sea-level budgets (Miller et al., 2020).
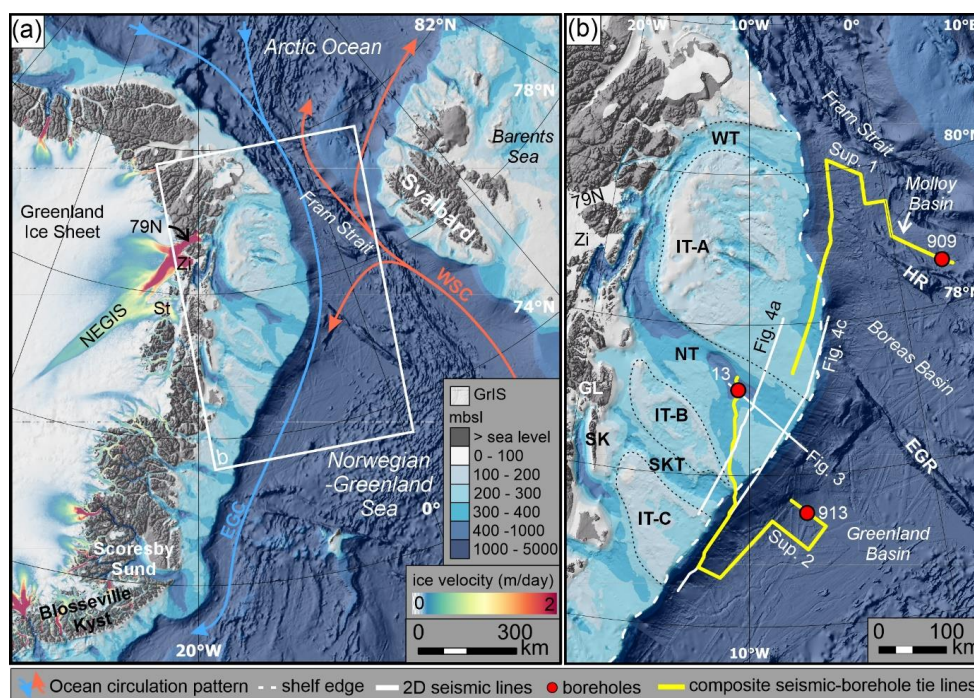
**Figure 1: a) Arctic and northern North Atlantic region with modern ocean circulation pattern indicated. EGC: East Greenland Current (cold). WSC: West Spitsbergen Current (warm). Ice velocity map of the Greenland Ice Sheet (GrIS) show the major Northeast Greenland Ice Stream (NEGIS) and its outlet glaciers; 79N: Nioghalvfjerdsbræ (79degreesnorthglacier). Zi: Zachariae Isstrøm. St: Storstrømmen. Topography and bathymetry compiled from IBCAO 5.0 (Jakobsson et al., 2024) and Arndt et al. (2015). Mbsl: meters below sea level. b) Northeast Greenland margin with locations of key seismic profiles and borehole data shown in this paper. Banks and troughs on the present-day shelf are annotated. WT: Westwind Trough. IT (A, B, C): Inter Trough area (A, B, C). NT: Norske Trough. SKT: Store Koldewey Trough. GL: Germania Land. SK: Store Koldewey. HR: Hovgaard Ridge. EGR: East Greenland Ridge.**

Ice streams are relatively narrow corridors within ice sheets that have a faster flow rate than adjacent areas, thus
60  despite covering a relatively small surface area, they account for the majority of the total ice drainage and discharge
from an ice sheet's interior to its margins (Dowdeswell & Elverhøi, 2002; Dowdeswell et al., 2006). As a result,
ice streams efficiently erode and transport sediments towards its terminus, shaping the landscape underneath them.
Marine terminating ice streams often operate within over-deepened cross-shelf troughs, carved out by this erosive
force. During long-lived glaciations, this erosive action creates large depocentres on upper slope beyond the ice
65  stream terminus, termed trough mouth fans (TMFs) (Vorren & Laberg, 1997; Batchelor & Dowdeswell, 2014).
TMFs thus serve as valuable geological archive that can be used to reconstruct former ice stream positions and
dynamics and thus the extent and evolution of former ice sheets.

This study uses a regional 2D seismic database that enables us to form the first coherent stratigraphic framework
from the upper Cenozoic strata across the entire outer NE Greenland margin (Fig. 2). Here, we describe the large-
70  scale architecture of the outer shelf and upper slope and present the regional long-term glacial history and evolution
based on geophysical mapping of TMFs buried in the geological record. We tie our improved stratigraphic
framework to three borehole sites which for the first time allow us to chronologically constrain the onset of shelf
glaciation across the NE Greenland shelf and major changes in ice sheet configuration.

75  ## 2    Regional setting

### 2.1    Study area

The Northeast Greenland margin between 75 – 81°N is characterized by a 700 km long continental shelf that
extends up to 300 km east of the coastline. The shelf in our study area is characterized by three over-deepened
cross shelf troughs that terminate at the shelf edge; Westwind Trough (WT), Norske Trough (NT) and Store
80  Koldewey Trough (SKT), separated by intermediate shallow banks (IT-A, B, C; Fig. 1). Westwind Trough and
Norske Trough are 300 – 430 km long, 40 – 200 km wide, and 200 – 500 m deep. The two troughs merge by the
coast at the outlet of the contemporary NEGIS (Fig. 1a), forming a ~~coherent~~ horse-shoe shaped trough encircling
the large inter-trough area IT-A; a complex of shallow banks and smaller depressions (water depths 2 – 400 m;
Fig. 1). The hummocky seafloor of IT-A has been attributed to salt tectonics causing folding and doming of
85  overlying strata and locally the salt diapirs sub-crop the seafloor (Hamann et al., 2005; Arndt et al., 2015; Fyhn et
al., 2021). Store Koldewey Trough (SKT) is 250 – 400 m deep, 200 km long and 30 – 50 km wide, located between
the shallow IT-B bank (150 – 250 m deep) and IT-C bank (50 – 150 m deep) to the north and south, respectively.
Store Koldewey Trough does not presently have any direct landward fjord or ice stream connection, but instead
abruptly initiates just off the coast of Germania Land and Store Koldewey island (Fig. 1). However, Olsen et al.
90  (2020) suggested that Storstrømmen glacier (St), a tributary of NEGIS presently terminating about 100 km west
of Store Koldewey, drained towards Store Koldewey Trough during the last glaciation (Fig. 1).
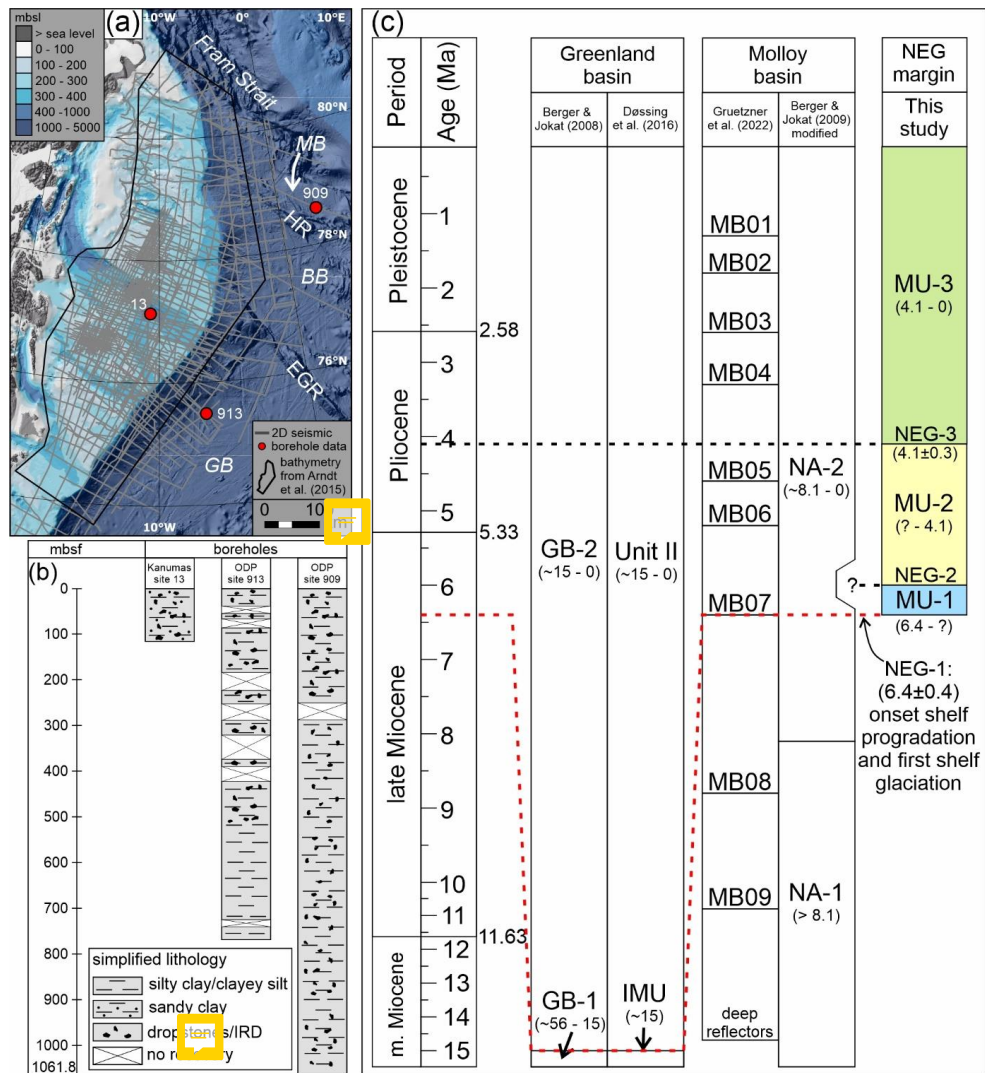
**Figure 2: a)** Coverage of bathymetry, borehole data and seismic data used in this study. MB: Molloy Basin. BB: Boreas Basin. GB: Greenland Basin. HR: Hovgaard Ridge. EGR: East Greenland Ridge. **b)** Simplified lithological description of the cores used in this study compiled from published data and reports. Mbsf=meters below seafloor. **c)** Chronostratigraphic overview of the outer Greenland margin, focusing on the presently established chronology in Greenland Basin (Berger and Jokat, 2008; Døssing et al., 2016), Molloy Basin (Berger and Jokat, 2009; Gruetzner et al., 2022) and their correlation to this study (dashed lines). The age of the boundaries from Berger & Jokat (2009) have been adjusted using the new age model from Gruetzner et al. (2022). NEG: Northeast Greenland. IMU: Inter-Miocene unconformity. Seismic data made available for this study courtesy of TGS, GEUS and GNPDR.

The shelf edge is located between 100 – 300 km from the coast and marks the boundary between the continental shelf and a relatively steep continental slope lacking any large-scale sliding, leading to the adjacent deep ocean Molloy Basin, Boreas Basin and Greenland Basin, reaching to approximately 2500 m, 3000 m and 3500 m water depths respectively. The deep ocean basins are themselves separated by fracture zones and structural highs at the Hovgaard Ridge and East Greenland Ridge (Fig. 1) which complicates direct seismic correlation between them (Hamann et al., 2005; Døssing et al., 2016).

## 2.2 Tectonic setting

The NE Greenland continental margin has been dominated by intense rifting since the onset of the late Paleozoic orogenic collapse, leading to formation of deep rift basins and structural highs now filled in by km-thick sedimentary sequences of late Paleozoic to early Cenozoic age (Hamann et al., 2005; Fyhn et al., 2021). The rifting culminated with the onset of seafloor spreading in the Norwegian-Greenland Sea during early Eocene, coinciding with tectonic compression (53 – 47 Ma), transpression (47 – 34 Ma) and finally rifting (34 Ma – recent) between northern Greenland and Svalbard margin (Piepjohn et al., 2016; Peron-Pinvidic & Osmundsen, 2018; and references therein). The Arctic Ocean was confined by shallow continental shelves until the earliest Oligocene when seafloor spreading eventually commenced between Svalbard and NE Greenland, in the present day Fram Strait (Kristoffersen, 1990; Engen et al., 2008). A narrow and possibly shallow oceanic gateway between the Norwegian-Greenland Sea and the Arctic Ocean through the Fram Strait was established by early Miocene (20 – 15 Ma), for the first time allowing circulation between the two oceans (Kristoffersen, 1990; Jakobsson et al., 2007; Engen et al., 2008). The onset of deep-water circulation through Fram Strait is uncertain, however, the gateway was probably not fully developed until late Miocene times (c. 9.8 Ma) as notified by seafloor spreading anomalies (Kristoffersen, 1990; Engen et al., 2008). Seafloor spreading in the Fram Strait coincides with two phases of tectonic uplift of the eastern Greenland margin in late Miocene (~10 Ma) and early Pliocene (~5 Ma) (Japsen et al., 2014; Døssing et al., 2016; Bonow & Japsen, 2021; and references therein), leaving eastward tilted and truncated inner shelf sedimentary successions that sub-crop the seafloor (Hamann et al., 2005; Fyhn et al., 2021).

## 2.3 Glacial history

The most recent (Late Weichselian) glaciation of the Northeast Greenland shelf reached its maximum extent during the Last Glacial Maximum about (about 24 – 16 Ka) (e.g., Funder et al., 2011), however the geometry, dynamics and extent of the GrIS across the shelf are still debated. Tributary ice streams of the NEGIS are suggested to have extended all the way to the shelf edge within the present-day Westwind Trough, Norske Trough and Store Koldewey Trough, as indicated by mapping of glacial landforms on the seafloor (Arndt et al., 2017; Laberg et al., 2017; Olsen et al., 2020; Ó Cofaigh et al., 2025). Whilst preserved mega-scale glacial lineations situated between recessional moraines and grounding zone wedges in the troughs have been suggested to indicate a rapid but episodic retreat pattern of the GrIS across the shelf during the last deglaciation (López-Quirós et al., 2024). Maximum extent and retreat dynamics across the bank is less certain, with suggestions that the outer shelf on the IT-A bank remained ice free through the last glaciation (Rasmussen et al., 2022).

Far less in known about the long-term glacial history the Northeast Greenland shelf. Evidence of circum-Arctic glacial ice is found in middle to late Miocene marine sediment records from the northern North Atlantic and the Norwegian-Greenland Sea. These findings show more or less continuous occurrences of ice rafted debris (IRD) since 12.6 – 10.8 Ma, consistent with circum-North Atlantic ice masses, including Greenland, reaching the coastlines frequently this time (Fronval & Jansen, 1996; Helland & Holmes, 1997; Knies & Gaina, 2008; Thiede, 2011; Gruetzner et al., 2022). Although the NE Greenland sector is not explicitly pointed out as the source area, this provides strong evidence that glacial ice did exist in Greenland at the time.

145 Seismic investigations offshore NE Greenland has identified massive prograding and gently inclined seismic sequences of late Cenozoic age within the shallowest stratigraphic interval on the outer shelf (Hamann et al., 2005; Berger & Jokat, 2008; Døssing et al., 2016). These prograding sequences rests on top of steeply inclined clinoforms and aggrading strata interpreted to represent deltaic sequences and submarine fans of assumed Eocene to Miocene age (Fig. 3) (Petersen, 2021). The prograding sequences are thought to represent increased sediment supply and

150 offshore sedimentation rates caused by localized glaciers onshore NE Greenland starting around 15 Ma (Berger & Jokat, 2008). However, age control here is based on seismic-borehole correlation to ODP Site 913, which is in turn poorly constrained for that time period (Myhre et al., 1995; Hull et al., 1996). Conversely, Petersen (2021) attributes the same prograding sequences to changes in sea level stands driven by uplift, subaerial erosion and subsequent fluvial and marine deposition along the outer palaeo-shelf, and speculates that the onset for shelf

155 glaciation occurred during the Plio-Pleistocene transition (c. 2.7 Ma). Hence, the precise timing and extent of grounded ice on the NE Greenland continental shelf remain unresolved, and the driving force behind significant shelf progradation is still debated.

During the last decades, the coverage of seismic datasets from this vast shelf area has increased, offering a new opportunity to study its glacial history. In this study we use these datasets to characterise the nature and thickness

160 the glacial sediment packages and constrain their age through ties to the few available boreholes, providing new information on the onset and evolution of shelf-edge glaciations along the NE Greenland continental margin.

### 3    Data & methods

This study uses a large 2D seismic dataset to improve the regional seismic stratigraphic framework, integrated

165 with published data from drilled sediment cores to chronologically constrain the glacial evolution of the NE Greenland margin (Fig. 2). The topographic and bathymetric background data used in this study are a composite of the IBCAO 5.0 (Jakobsson et al., 2024) and interpolated bathymetry from Arndt et al. (2015) (Fig. 2a). The extent of the present-day GrIS and its velocity are respectively derived from BedMachine v5 by Morlighem and et al. (2022) and ice velocity map acquired through the Cryoportal (Nagler et al., 2015).

170

### 3.1    Seismic data

This study uses 46 000 km of 2D reflection seismic data covering most of the NE Greenland margin, an area of more than 200 000 km$^2$ (Fig. 2). The data consists of multiple surveys acquired by both industry and academia between 1994 – 2014, with considerable variations in acquisition parameters and material used (Table 1). The

175 dominant frequency of each dataset are used to calculate the dominant wavelength and resolution assuming an average velocity of 1500 m/s at the seafloor as used in comparable settings (e.g., López-Quirós et al., 2024). The resulting vertical resolution of the seismic data, estimated for the seafloor, ranges between c. 16.5 m – 47 m (Table 1).

**Table 1: An overview of seismic surveys used in this study and their vertical resolution at the seafloor based on an average sound velocity of 1500 m/s. *The AWI surveys used here were reprocessed by TGS in 2010.**

| Acquired by | Year | Source | Streamer (m) | Vertical resolution at seafloor (m) |
|---|---|---|---|---|
| Kanumas Group | 1994 | Airgun 2050 in³ | 1500 | 16.5 |
| Kanumas Group | 1995 | VSX Airgun 2050 in³ | 2100, 1500 | 21 |
| AWI* | 1999 | Airgun 5x9L | 1700 | 19 |
| AWI* | 2002 | Airgun VLF 24l | 600 | 23.5 |
| AWI* | 2003 | VLF-Gunsx3l & G-Gunsx8.5l | 600, 3000 | 19 |
| Norsk Hydro | 2006 | Airgun | 6000 | 22 |
| TGS | 2008 | Airgun | 6000 | 19 |
| TGS | 2009 | Airgun | 6000 | 19 |
| TGS | 2011 | Airgun, 1500LL & 1900LLX | 3000 | 25 |
| TGS | 2013 | Airgun 3350 in³ | 4500, 6000 | 37.5 |
| TGS | 2014 | Airgun 1675 – 3350 in³ | 6000 | 47 |
| GXT | 2009 | Airgun 4330 in³ | 8000 | 37.5 |
| GXT | 2010 | Airgun 4330 in³ | 8000, 6000 | 37.5 |
| GXT | 2011 | Airgun 4330 in³ | 8000 | 37.5 |

### 3.2 Borehole data

Published data from Ocean Drilling Program (ODP) Leg 151 Sites 909 and 913 (Myhre et al., 1995) are used to provide sedimentological and chronological constraints on the regional seismic stratigraphic units from this study. We apply the revised chronology by Gruetzner et al. (2022) for Site 909, and use the chronology by Hull et al. (1996) at Site 913. The summary report from the NE Greenland Stratigraphic Coring project 2008 (StatoilHydro, 2008) is used to provide sedimentological information from Kanumas Site 13, located on the NE Greenland shelf.

#### 3.2.1 ODP Site 909

ODP Site 909 is located at 2519 m water depth in the Molloy Basin, central Fram Strait (Fig. 2) (Myhre et al., 1995). The site penetrated a total of 1061.8 meters of sediments, corresponding to a true vertical depth of 1023 meters below seafloor (mbsf) after correcting for deviation of the drill pipe (Myhre et al., 1995). We apply the newest age model for this site by Gruetzner et al. (2022), providing an upper middle Miocene age (13.8 – 11.6 Ma) to the base of Site 909 (Fig. 2c). The site mainly recovered clay and silty clay sediments with common occurrences of large dropstones in the upper 240 mbsf (Fig. 2b) (Myhre et al., 1995). IRDs were described from

the whole core, spanning from upper middle Miocene to late Pleistocene (Fig. 2b) (Winkler et al., 2002; Knies & Gaina, 2008; Thiede, 2011; Gruetzner et al., 2022).

### 3.2.2 ODP Site 913

200 ODP Site 913 is located at 3318 m water depth in the Greenland Basin c. 100 km east of the NE Greenland shelf (Fig. 2a). We use the age model from Hull et al. (1996). The borehole reached a total depth of 770.3 mbsf, retrieving early Eocene to late Pleistocene sediments. However, the upper 423 m of the core, corresponding to the Miocene to present stratigraphic interval, suffered from very poor recovery, limiting the age constraints for this period (Fig. 2b) (Myhre et al., 1995). The core has generally been described as clayey silt to silty clay with up to

205 cobble-size dropstones in the upper c. 380 m. The deepest IRDs has been described down to a depth of c. 550 mbsf, corresponding to Eocene-Oligocene (Eldrett et al., 2007; Tripati et al., 2008).

### 3.2.3 Kanumas Site 13

The NE Greenland Stratigraphic Coring Project was a commercial coring project carried out in 2008 by the

210 Kanumas group (Lundin, 2013), targeting shallow sub-cropping seismic stratigraphic intervals of commercial interest. Kanumas Site 13 is located on the shelf within Norske Trough at 509 m water depth, about 100 km from the shelf edge (Fig. 2a). The description given here is based on the summary report which provided lithological descriptions and photographs of the whole core (StatoilHydro, 2008). The borehole reached a total depth of 114.9 mbsf, recovering a total of 91.9 m of sediments (82% recovery). The entire core was generally described as sandy

215 clay with stones of varying size, shape and composition, only interrupted by short (≤1 m) laminated intervals (Fig. 2b, S1). No age information for this core is presently available.

### 3.3 Methods

### 3.3.1 Seismic interpretation

220 The 2D seismic data presented in this study have been compiled, interpreted and tied to borehole data in commercial software. The TGS surveys were used as reference when adjusting for vertical offset between seismic surveys. Strong multiples occur in some seismic data which can be problematic on the shelf areas, especially when interpreting horizontal reflections. To avoid falsely picking these multiples, duplicate time-surfaces of the seafloor reflection was shifted vertically (2x, 3x, 4x) to show where the multiple would be in the seismic data.

225 This study has focused on interpreting reflections that represent regional unconformities in the seismic record, marking the boundaries for large scale changes in depositional pattern. We have adopted the reflection terminology of Mitchum et al. (1977) to describe the seismic facies and termination pattern of individual reflections. Specific horizons have been tracked manually and using supervised 2D-assisted tracking. Three regional unconformities were identified in this study with time surfaces created for each horizon using a 1 km grid size. The regional

230 reflections represent the boundaries of three major seismic units (MU-1 – MU-3). The isochron thickness of each unit was calculated by subtracting the lower surface from the upper one for each unit and are given in two-way

travel time (TWT). The resulting surfaces and thickness maps were further analysed and visualized using ArcGIS Pro.

### 3.3.2    Seismic-borehole tie

Available velocity profiles from ODP Site 909 (Gruetzner et al., 2022), Site 913 (Myhre et al., 1995), and a velocity model of the NE Greenland shelf (Berger & Jokat, 2008) have been used to tie the boreholes to the seismic data and to match the interpreted seismic horizons. The available velocity profile from ODP Site 909 (Gruetzner et al., 2022) yields an average velocity of 1.66 km/s for the interval c. 0 – 350 mbsf, and 1.98 km/s for the interval 350 – 650 mbsf. Here, we implement the average velocities for each interval to convert the borehole depth (mbsf) to two-way travel time (TWT). The average velocity at Site 913 was reported by Myhre et al. (1995) to be varying between 1.48 – 1.82 km/s, with the exceptions of carbonate concretions and the very deepest part which exceeded 2.0 km/s. Here, we use 1.66 km/s as an average velocity when converting Site 913 borehole depth to TWT. Likewise, seismic velocity analysis by Berger and Jokat (2008) suggests a velocity of 1.5 km/s to 1.7 km/s for the upper c. 500 m of the subsurface on the shelf, thus, we use an average subsurface velocity of 1.66 km/s (similar to Site 913) to convert Kanumas Site 13, located on the shelf, from borehole depth to TWT (Fig. 1b).

## 4    Results and interpretation

We identify three major reflections that represent regionally unconformable boundaries that can be correlated across the Northeast Greenland (NEG) margin (Figs. 3, 4). From bottom to top, these reflections are named NEG-1 to NEG-3 and correlate with chronological intervals between the late Miocene to late Pliocene. Furthermore, the reflections define three seismic mega units (MU) to be described below.

**Table 2: Seismic-borehole tie-depths for the key reflections from this study. Vertical tie-depth is given in meters below seafloor (mbsf) with an uncertainty equal to the vertical resolution of the seismic tie-line (table 1). Age estimates from ODP Site 909 and 913 are based on the age models by Gruetzner et al. (2022) and Hull et al. (1996), respectively. *Estimated age by this study. **Estimated depth below Kanumas Site. TWT=two-way travel time in seconds.**

| Horizon | Tie depth TWT (s) | Borehole site | Depth in borehole (mbsf) | Age estimations (Ma) | Chronology |
|---------|-------------------|---------------|--------------------------|----------------------|------------|
| Seafloor | 3.407 | **ODP Site 909** | 0±23.5 | 0 | |
| NEG-3 | 3.78 | | 310±23.5 | 4.1±0.3 Ma | early Pliocene |
| NEG-1 | 4.13 | | 652±23.5 | 6.4±0.4 Ma | late Miocene |
| Seafloor | 4.5 | **ODP Site 913** | 0±19 | 0 | |
| NEG-3 | 4.76 | | 215±19 | 5.3 – 0 Ma | Plio-Pleistocene |
| NEG-1 | 4.99 | | 405±19 | 16 – 5.3 Ma | mid/late Miocene |
| Seafloor | 0.684 | **Kanumas Site 13** | 0±16.5 | 0 | |

| NEG-2 | 0.72 | | 30±16.5 | 6.4 – 5.3 Ma?* | late Miocene?* |
| NEG-1** | 0.83** | | 122±16.5** | - | late Miocene |
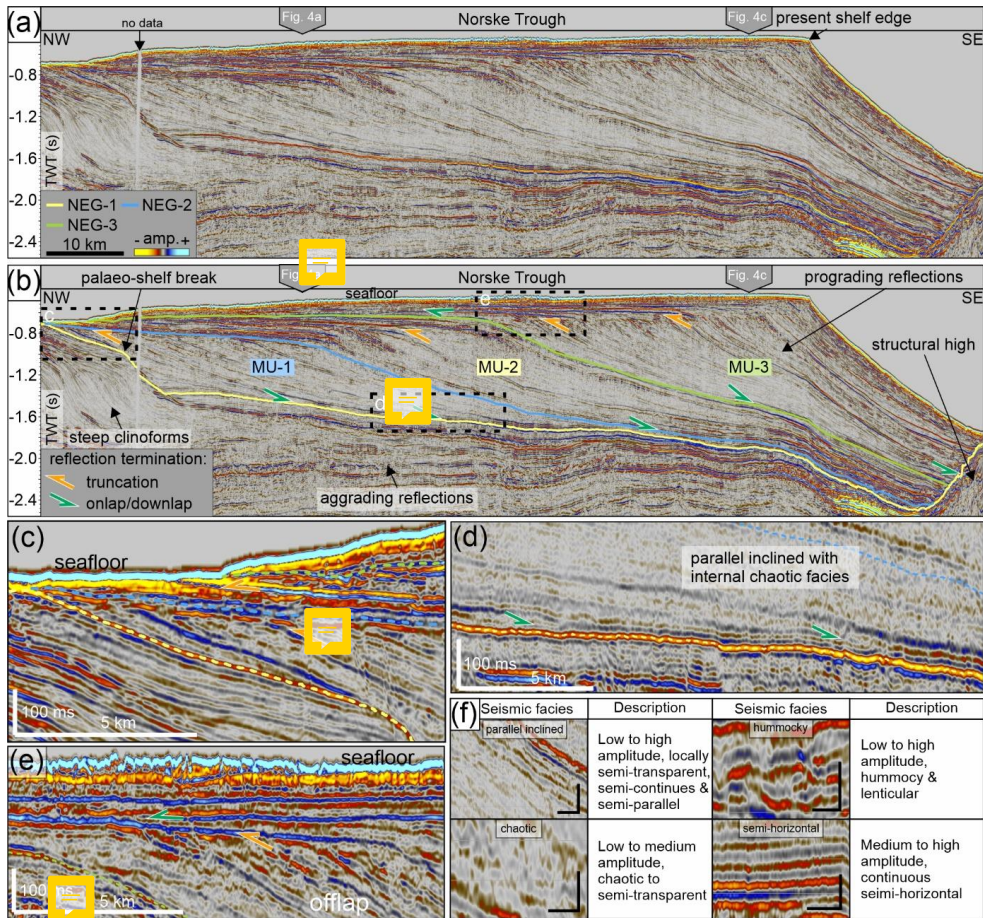
**Figure 3: Cross-shelf oriented seismic profile from Norske Trough (see Fig. 1 for location). a) Uninterpreted seismic profile. Grey wide arrows locate the cross-seismic lines in Fig. 4 for reference. TWT=two-way travel time. b) Key regional reflections and internal reflection termination pattern. MU=Mega Unit (-1, 2, 3). c) Zoomed in view on the palaeo-shelf break and onset of shelf progradation. d) Reflection termination pattern at the base of the prograding units. e) Truncated foresets and onlapping topsets. f) Examples and descriptions of key seismic facies described in this study. Scalebar: Vertical axis 50 ms (TWT). Horizontal axis 1 km. Seismic courtesy of TGS.**
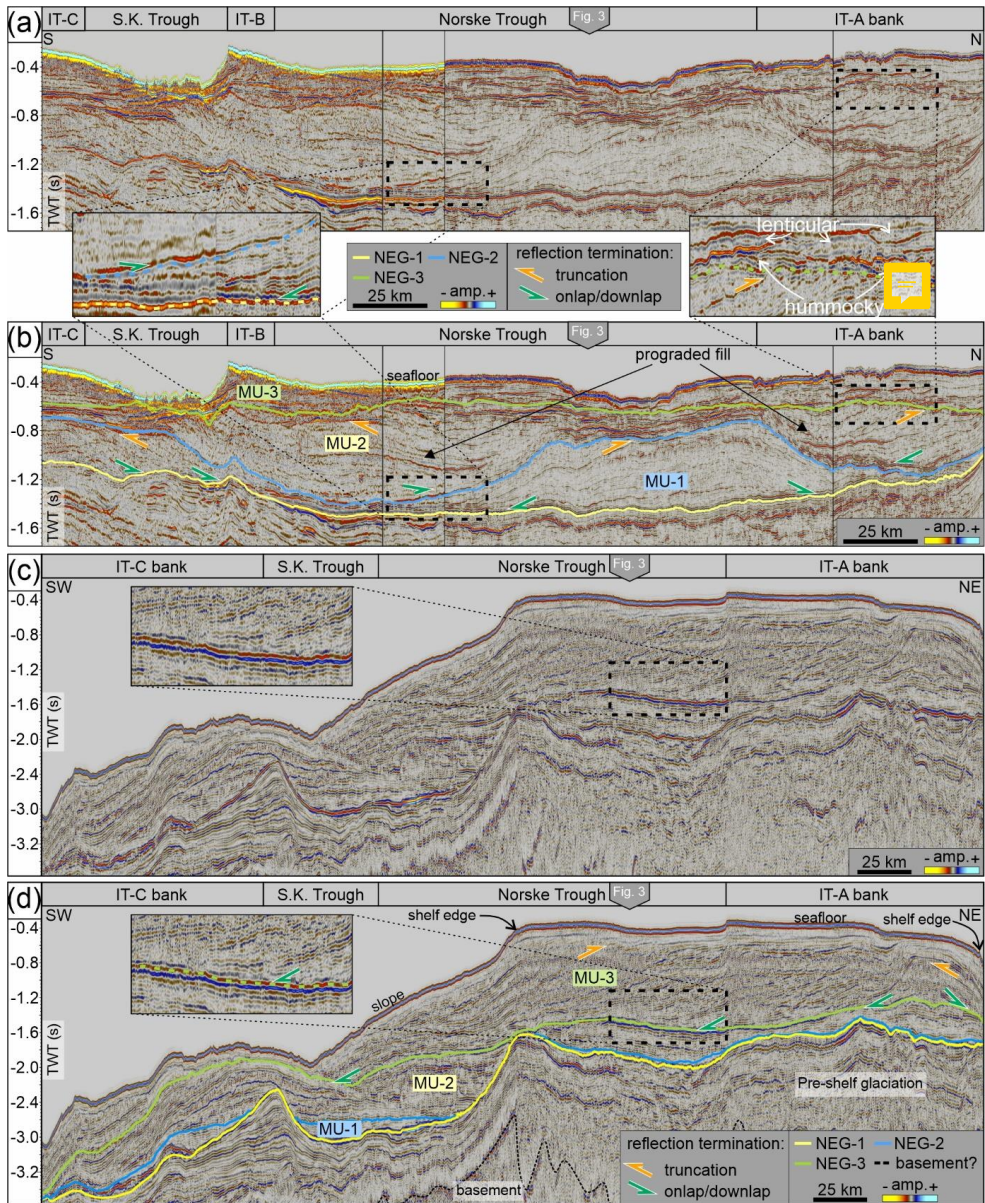
260

**Figure 4: Along-shelf oriented seismic profiles from the central shelf (a & b) and outer shelf/upper slope (c & d; see Fig. 1 for locations), with present-day shelf-corresponding troughs and banks annotated for reference. Grey wide arrows locate the cross-seismic line in Fig. 3 for reference. a) Uninterpreted composite seismic profile. Insert figures show examples of seismic facies and reflection terminations as described in the results. b) Interpretation of composite seismic line a. Note the indicated prograding fill pattern north and south of MU-1 in Norske Trough. c) Uninterpreted seismic profile with insert figure to show general reflection termination pattern at this interval. d) Interpretation of seismic line C. MU=Mega Unit (-1, 2, 3). S.K. Trough= Store Koldewey Trough. Seismic courtesy of GEUS and GNPDR.**

### 4.1 Regional reflections

#### 4.1.1 Regional Unconformity (late Miocene: 6.4 Ma)

The Northeast Greenland Regional Unconformity (NEG-1) is regionally recognized as a reflection of high amplitude and reverse polarity compared to the seafloor (Figs. 3, 4). The reflection marks a regionally unconformable boundary that can be traced across the entire study area. On the outer shelf it separates underlying (generally conformable) aggrading strata from the overlying prograding strata that (unconformably) terminate by downlap onto NEG-1. Landwards, on the central and inner shelf, NEG-1 truncates underlying tilted aggrading strata, whereas it is conformable to overlying semi-horizonal to hummocky reflections (landward component of the prograding reflections).

Correlation of NEG-1 into the Molloy Basin and ODP Site 909 shows that it ties with Site 909 at about 652 mbsf, corresponding to a late Miocene age of 6.4±0.4 Ma according to the revised age model by Gruetzner et al. (2022) (Table 2, Figs. 5a-e, S2). This age is supported by our correlation to Site 913 in the Greenland Basin where NEG-1 ties at 405 mbsf, corresponding to the upper part of subunit IIIa which is estimated to be of mid to late Miocene age (Myhre et al., 1995; Hull et al., 1996) (Table 2, Figs. 5f-I, S3).

NEG-1 has been correlated across most of the NE Greenland margin, for about 800 km from Westwind Trough (WT) and Molloy Basin in the north to IT-C bank and Greenland Basin in the south, and up to 400 km from the inner continental shelf in the west to the deep ocean basins in the east (Fig. 6a). The interpolated time-surface of NEG-1 expresses a palaeo-shelf with a sharp offlap marking the palaeo-shelf break position up to 100 km west of the present-day shelf edge within Norske Trough (NT) and Store Koldewey Trough (SKT) (Fig. 6a, 6d). Further north along the outer IT-A bank and Westwind Trough, the difference in shelf-width compared to its present-day position decreases to 10 km – 40 km. Three slightly over-deepened cross-shelf troughs can be recognised on the palaeo-shelf, located below the contemporary troughs. Westwind Trough has a similar width to its contemporary part whereas Norske Trough and Store Koldewey Trough both seem to be wider on the outer palaeo-shelf, compared to the present-day troughs. East of the NEG-1 palaeo-shelf edge, a buried submarine plateau is located below the outer Norske Trough and Store Koldewey Trough, between the palaeo-shelf edge and the present-day shelf edge. Ridges and structural highs are visible east and southeast of the present-day shelf edge, as the time-surface deepens towards the basins.

#### 4.1.2 Semi-regional reflection (late Miocene?)

The ~~semi-regional~~ reflection, termed NEG-2, is stratigraphically situated above NEG-1 and marks a ~~semi-regional~~ ==reflection== that truncates underlying prograding reflections (Figs. 3, 4a, 4b). The ~~reflection~~ is characterized by a medium amplitude, and it is a continuous reflection that towards the east terminates by downlap onto NEG-1. Its western extent is limited to the palaeo-shelf edge of the NEG-1 surface where it either onlaps onto NEG-1, is truncated by overlying reflections or becomes too thin to be resolved by the seismic data (Fig. 3). NEG-2 ties at 30 mbsf with the Kanumas borehole at Site 13 located on the shelf (Table 2, Figs. 5j-l, S1). However, the Kanumas Site 13 does not provide any age constraints and NEG-2 has not been possible to correlate to any of the ODP sites.

NEG-2 represents a semi-regional reflection that has been identified between 79°N – 75°N and 15°W – 5°W, extending about 500 km across entire outer Norske Trough and Store Koldewey Trough and the adjacent bank

areas, and 200 km from the palaeo-shelf edge in the west to the lower slope and rise in the east (Fig. 6b). The time-surface of NEG-2 shows shelf expansion beyond that of NEG-1 at two distinct locations. The most pronounced shelf development is a c. 100 km wide area at the central-northern Norske Trough where the shelf propagates about 40 km towards the southeast in a fan-like shape, forming a bulge in the palaeo-surface (Fig. 6b). The top of the fan is flattened with a low relief SE-NW oriented trough central to it. The second distinct shelf expansion of up to 60 km towards SE occurs within a c. 150 km broad area on the outer IT-C bank and Store Koldewey Trough, where parts of it correspond to the present-day shelf edge position (Fig. 6b).
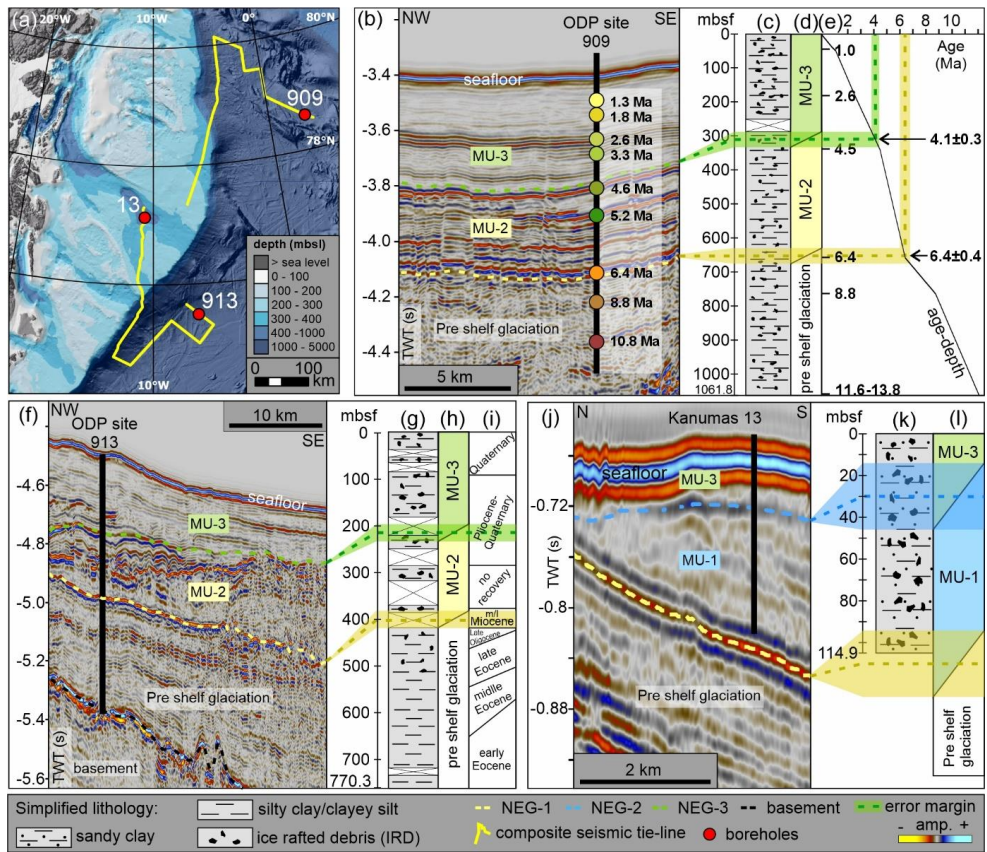
**Figure 5: Seismic-borehole ties from this study shown by coloured dashed lines with transparent background (error margins). Legends are shared with all figures. Horizontal transparent error margins represented by seismic vertical resolution (m) (note scale differences in borehole logs; see table 1). a) Location of composite seismic tie-lines (yellow lines) used to regionally correlate reflections from the shelf towards the deeper basins and the boreholes (red circles). b) Seismic-borehole tie at ODP site 909 with annotated assigned ages for major seismic reflections modified from Gruetzner et al. (2022). c) Simplified lithological description of ODP site 909. d) Depth-correlation of regional seismic reflections and mega units (MU) to site 909 (dashed lines). e) Age-depth model for site 909 with age fix points (Ma) on vertical axis from Gruetzner et al. (2022). Vertical transparent error margin represents the age uncertainty for each tie-depth. f) Seismic-borehole tie at ODP site 913. g) Simplified lithological description of ODP site 913. h) Depth-correlation of our seismic reflections and mega units to site 913. i) Age model for site 913 by Hull et al. (1996). j) Seismic-borehole tie at Kanumas site 13. Note that the borehole did not reach the NEG-1 reflection boundary. k) Simplified lithological description of Kanumas site 13. l) Depth-correlation of our seismic reflections and mega units to site 13. Seismic courtesy of TGS, GEUS and GNPDR.**

### 4.1.3     Pliocene Unconformity (early Pliocene: 4.1 Ma)

The NEG-3 reflection is stratigraphically situated between the NEG-2 reflection and the present-day seafloor. It is characterized by a strong continuous reflection with an opposite polarity to that of the seafloor (Figs. 3, 4). The

335    reflection marks a distinct unconformable boundary at the outer Norske Trough and adjacent upper slope where overlying prograding reflections terminate by downlap onto NEG-3, whereas underlying reflections has a conformable relation to it (Fig. 4c-d).

NEG-3 is correlated to ODP Site 909 in the Molloy Basin. The reflection ties with Site 909 at about 310 mbsf, corresponding to a mid-Pliocene age of 4.1±0.3 Ma when plotted against the age model by Gruetzner et al. (2022)

340    (Table 2, Figs. 5b-e, S2). This is supported by our correlation into the Greenland Basin and ODP Site 913 where NEG-3 ties at 215 mbsf corresponding to an interval suggested to be of Plio-Pleistocene age (Myhre et al., 1995; Hull et al., 1996) (Table 2, Figs. 5f-I, S3).

NEG-3 is here correlated along most of the outer shelf and slope for about 750 km from Westwind Trough to IT-C bank and for 200 km to 300 km from the palaeo-shelf edge (NEG-1) into Molloy and Greenland Basins (Fig.

345    6c). The surface expression of NEG-3 shows a further expansion of the shelf of up to 50 km towards SE along about c. 300 km of the outer Norske Trough and Store Koldewey Trough and adjacent banks, forming a straightened NE-SW oriented palaeo-shelf break. Consequently, NEG-3 completely buries the submarine plateau as seen on the surface of NEG-1 and now forms a relatively even slope angle towards the Greenland Basin. NEG-3 also show expansion along c. 150 km of the shelf further north on the northern part of IT-A bank and at the outer

350    Westwind Trough, although to a lesser degree than that of Norske Trough.

## 4.2     Seismic Units

The regional reflections described above define the base and top of three seismic mega units (MU-1 to MU-3). From bottom to top, these mega units correlate with time intervals from late Miocene to recent as determined by

355    regional correlation of the reflections. Combined, these three mega units form a coherent deposit along the entire outer shelf with a maximum isochron (time) thicknesses between 0.8 s – 2.0 s (TWT) below the present-day shelf edge (Figs. 6e, S4a).

### 4.2.1     Mega Unit-1 (late Miocene)

360    The lowermost seismic mega unit (MU-1) is bounded by NEG-1 and NEG-2 at its base and top respectively (Fig. 6f). It is characterized by seaward progradation of parallel reflections separating intervals of chaotic to transparent seismic facies (Figs. 3, 4). The reflections taper out towards the east and terminate by downlap onto NEG-1, whereas the top of the prograding reflections is clearly truncated by NEG-2. Two depocentres can be recognized from the isochron thickness map of MU-1 (Figs. 6f, S4b), corresponding to the distinct seaward buildout of the

365    shelf

as seen in the NEG-2 surface map (Fig. 6b). Both depocentres measure about 0.75 s (TWT) and are located on the outer part of Norske Trough and Store Koldewey Trough/IT-C, just seaward of the palaeo-shelf break of NEG-1. The rest of MU-1 is composed of ≤0.25 s thick eastward thinning sequences.

The cored interval between 30 – 114.9 mbsf at Kanumas Site 13 corresponds to the lowermost part and the onset

370    of MU-1 (Figs. 5j-l, S3). This interval is dominated by a silt-borne diamictite interbedded with short intervals (<1

m) of laminated silt-dominated sediments (StatoilHydro, 2008).
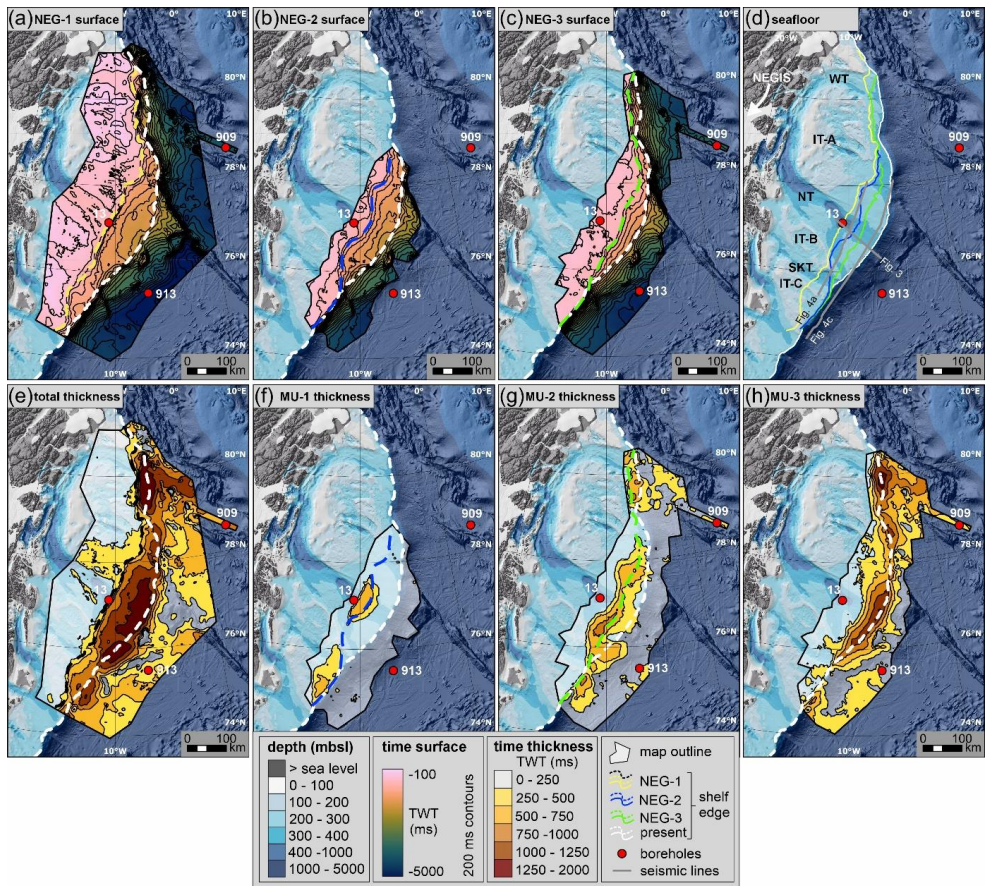
**Figure 6: Interpolated surfaces and isochron thickness maps shown in two-way travel time (TWT). Palaeo-shelf edge positions for each respective surface/map is shown by coloured dashed lines. Present-day shelf edge shown in white dashed line. Shared legends for all maps located above. a) Interpolated surface of NEG-1 and its interpreted extent. b) Interpolated surface of NEG-2 and its interpreted extent. c) Interpolated surface of NEG-3 and its interpreted extent. d) present-day seafloor with indicated palaeo-shelf edge positions for all three reflections. e) Total thickness map measured from NEG-1 to the seafloor reflection. f) Thickness map of MU-1, measured from NEG-1 to NEG-2. g) Thickness map of MU-2, measured from NEG-1+NEG-2 to NEG-3. h) Thickness map of MU-3, measured from NEG-3 to the seafloor reflection. MU=Mega Unit (-1, 2, 3).**

### 4.2.2    Mega Unit-2 (late Miocene – early Pliocene)

The middle seismic unit (MU-2) is defined by NEG-3 as its upper boundary, whereas the lower boundary is defined by NEG-2 in the outer part of Norske and Store Koldewey Trough and adjacent bank areas and defined by NEG-

385    1 outside the interpreted extent of NEG-2 (Figs. 6a-d, 6g). MU-2 is characterized by both seaward prograding

slope sequences and semi-horizontal to hummocky and lenticular top sequences. The prograding sequences are

generally characterized by alternating parallel and chaotic to transparent seismic facies, similar to that of MU-1

(Figs. 3, 4). The lower part of MU-2 forms a prograded fill pattern in the accommodation space above MU-1 and downlap onto NEG-2 on the inner part of the shelf (Fig. 4a-b). Eastward, the lower part of MU-2 downlap onto

390     NEG-1 whereas the upper parts thin towards east and becomes dominated by semi-parallel reflection characteristics that are generally draped onto and mimics the expression of NEG-1 (Figs. S1 and S2).

The isochron thickness map of MU-2 reveal two distinct depocentres (Fig. 6g, S4c) located at the: 1) outer Norske Trough and Store Koldewey Trough and adjacent bank areas from the southern IT-A bank to the outer IT-C bank. It measures up to 0.85 s (TWT) at its thickest at the southern part of Norske Trough, forming a prograding fill

395     deposit in the accommodation space between the two depocentres earlier described from MU-1. 2) A partly divided depocentre is located on the outer Westwind Trough and northern IT-A bank with a maximum isochron thickness up to 0.9 s (TWT). Parts of this depocentre extends towards the Molloy Basin.

If we combine the total shelf progradation of MU-1 and MU-2, which show a maximum of 68 km shelf progradation towards southeast, we can assert a maximum shelf progradation rate of about 29 km/Ma in the period

400     between 6.4 and 4.1 Ma.

### 4.2.3     Mega Unit-3 (early Pliocene – Recent)

Seismic unit MU-3 is the uppermost unit defined between NEG-3 and the seafloor reflection at its base and top, respectively, and corresponds to a mid-Pliocene to recent age (Figs. 3, 4, 5). The internal seismic characteristics

405     of MU-3 are similar to that of MU-2 and MU-1, generally consisting of seaward prograding slope sequences and semi-horizontal to hummocky and lenticular top sequences. The characteristics of the prograding sequence alternate between a parallel and chaotic to transparent signature. Analysis of internal reflections within this unit reveals that it represents a subtle shift in the prograding trajectory from southeast for MU-1 and MU-2 to south-southeast for MU-3. This is evident in along-shelf profiles as downlap-termination by internal reflections onto

410     NEG-3 and in cross-shelf profiles by a reduced spacing between individual reflections (Figs. 3, 4).

The isochron thickness map (Fig. 6h, S4d) show that this unit is a coherent, thick deposit stretching along the entire studied outer shelf, with its thickest parts positioned underneath the present-day shelf edge. Four distinct depocentres can be recognized: 1) The unit is at its thickest at the outer Westwind Trough and northernmost IT-A bank, measuring up to 1.4 s (TWT). The depocentre is slightly elongated oriented along shelf, with a tail of

415     increased thickness stretching into the Molloy Basin. 2) A slightly elongated fan-shaped depocentre oriented parallel to the shelf edge is located on the central outer IT-A bank, measuring up to 1.0 s (TWT) thickness. 3) A particularly elongated depocentre oriented along shelf in the outer Norske Trough and surrounding areas (IT-A and IT-B), measures up to 1.3 s (TWT) thickness. 4) The southernmost depocentre located on the slope outside of IT-C and Store Koldewey Trough, measures up to 1.1 s (TWT) thickness.

420     MU-3 has a maximum shelf progradation of about 61 km within outer Norske Trough, providing a maximum shelf progradation rate of about 15 km/Ma for the period 4.1 Ma to recent.

### 4.3 Interpretation: glaciogenic deposits

This study has mapped out three regional seismic mega units (MU-1 to MU-3) which are dominated by shelf
progradation. The mega units are bounded by key unconformable reflections (NEG-1 to NEG-3). NEG-1 is
interpreted as a regional unconformity that marks a shift from predominantly aggrading units below to major shelf
progradation above. In Norske Trough and towards the Greenland Basin, NEG-1 generally corresponds to a strong
unconformity interpreted by previous studies (Hamann et al., 2005; Berger & Jokat, 2008; Petersen, 2021; López-
Quirós et al., 2024), termed the Intra Miocene-Unconformity (IMU) by Døssing et al. (2016) (Fig. 2). In Molloy
Basin the NEG-1 reflection corresponds to MB07 identified by Gruetzner et al. (2022) (Figs. 2c, 5).

Kanumas Site 13 penetrates the lower part of seismic MU-1, documenting that this interval of inclined semi-
parallel and semi-continuous seismic facies is dominated by matrix borne diamictite (Figs. 5j-l, S1), consistent
with an ice-proximal depositional environment (Laberg & Vorren, 1995; Dowdeswell & Elverhøi, 2002). We
interpret the chaotic to semi-transparent seismic faces found within the prograding foresets as glaciogenic debris
flow deposits, indicating periods when glacial ice extended all the way to the palaeo-shelf edge during glacial
maxima conditions (Laberg & Vorren, 1996; Vorren & Laberg, 1997; Dahlgren et al., 2005). In line with this, we
interpret MU-1 to be of glacial origin, based on the fan-shaped geometry of the depocentres, their location within
cross-shelf troughs or in vicinity to troughs, internal seismic facies of inclined parallel to chaotic character which
core data indicates to be an ice-proximal sedimentary deposit. Similar characteristics of shelf prograding seismic
units have been interpreted to indicate historical shelf glaciations from both hemispheres (Cooper et al., 1991;
Laberg & Vorren, 1995; Nielsen et al., 2005). NEG-2 is interpreted as an erosional boundary that separates MU-1
from the overlying seismic mega units.

The aggrading medium to high amplitude topsets of hummocky/lenticular to semi-horizontal seismic character
observed in MU-2 and MU-3 are interpreted as alternating deformation till deposited during glaciations and
marine/glacimarine sediments deposited during interglacials and/or glaciations that did not reach the shelf edge.
Preserved aggrading topsets from other formerly glaciated shelves have been suggested to indicate syn-
depositional subsidence of the outer margin due to sediment loading (Dahlgren et al., 2002; Dahlgren et al., 2005),
a similar process may have facilitated preservation of aggrading topsets on the NE Greenland shelf. The prograding
foresets of MU-2 and MU-3 share characteristics to that of the underlying MU-1, and the thickness maps of both
units show that the main depocentres are elongated along-slope, have a fan shaped geometry and most are located
within cross-shelf troughs. We therefore interpret both MU-2 and MU-3 to be predominantly deposited during
shelf glaciations. NEG-3 is defined as a regional unconformity traced along the outer shelf to the adjacent basins.
It is interpreted to indicate a possible hiatus or condensed section prior to a major shift in ice sheet configuration
on the northeast Greenland shelf (Fig. 6f-h).

## 5 Discussion

### 5.1 NE Greenland Ice sheet development since the late Miocene

Based on the regional correlation of key seismic reflections across the NE Greenland margin we have identified
three seismic mega units that we interpret to reflect large scale ice sheet development on the NE Greenland shelf
since the late Miocene. This ice sheet development is characterized by changes in ice stream configuration across

the shelf, represented by distinct depocentres and shelf progradation, and are presented in our three-stage conceptual model (Fig. 7). In the following, we elaborate on our interpretations of each stage and discuss potential climatic and tectonic factors that have played a role in driving ice sheet changes since late Miocene. We ultimately compare our reconstruction of the long-time GrIS evolution with other ice sheets during this time period (Fig. 8).

465
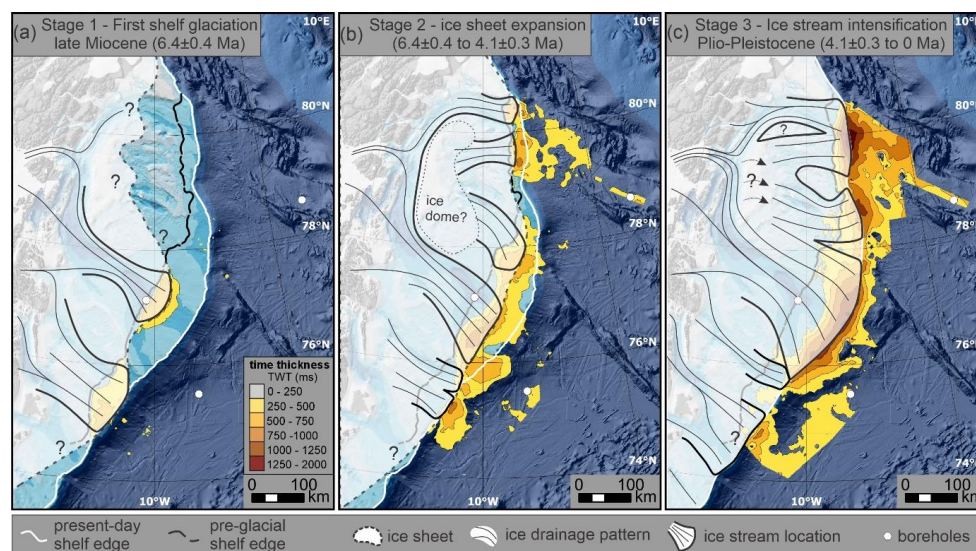
**Figure 7: Three stage conceptual sketch of the ice sheet configuration and drainage pattern on the NE Greenland shelf from late Miocene to Plio-Pleistocene. The ice sheet and respective ice streams are overlain on the time-thickness maps from this study. a) Stage 1 – the first shelf glaciation reaching the palaeo-shelf edge that can be observed in the seismic stratigraphic record, occurring around 6.4 Ma. b) Stage 2 – Between late Miocene to early Pliocene the ice sheet advanced multiple times across the shelf, with an expanded ice margin towards north and east compared to Stage 1. c) Stage 3 – Intensified ice streaming starts sometime after 4.1 Ma, indicated by major changes in ice sheet configuration and frequent shelf glaciations of the Greenland Ice Sheet.**

470

### 5.1.1    Stage 1 – First shelf-edge glaciation (6.4 Ma)

475    Here we interpret MU-1 to mark the first recorded advance of grounded ice masses across the NE Greenland shelf (Fig. 7a). The sedimentological descriptions, internal seismic facies and fan-shaped morphology of the MU-1 depocentres are all characteristic of trough mouth fans (TMFs), formed at the terminus of former ice streams reaching the shelf edge. These ice streams deposit vast amounts of glaciogenic sediments at their margin which are subsequently reworked downslope. This is a repeating cycle causing progradation of the shelf over multiple

480    glaciations and is seen on both formerly and contemporary glaciated shelves (Laberg & Vorren, 1995, 1996; Vorren & Laberg, 1997; Dahlgren et al., 2005; Nielsen et al., 2005; Nygård et al., 2005). MU-1 is constrained to a maximum age of 6.4±0.4 Ma, which corresponds to the onset of increasing IRD input to the Fram Strait, peaking at around 6 Ma (Fig. 8) (Gruetzner et al., 2022).

The two TMFs of MU-1 are laterally constrained to the central-northern part of Norske Trough and to the southern

485    part of Store Koldewey Trough and outer IT-C bank (Figs. 6b, 6f). This suggests that the location of active ice streaming was relatively stable during deposition of MU-1, possibly constrained by the pre-glacial topography. The thickness map of MU-1 indicates that the ice streams operating in Norske Trough and Store Koldewey Trough,

feeding these TMFs, may have been up to 100 - 150 km wide. Given their similarity to other large TMFs described
around the Greenland and Barents Sea margins (Vorren & Laberg, 1997; Batchelor & Dowdeswell, 2014), this
490  suggests a similar dimension of ice streaming during late Miocene as to that of Plio-Pleistocene ice streams.
Between the two TMFs is a thin but continuous deposit with minor shelf progradation along the palaeo-shelf edge.
This is here interpreted to indicate a coherent ice margin reaching the shelf edge at the IT-B bank, between the two
ice streams, although, possibly dominated by stagnant, cold based ice that prevented active ice streaming (Fig 7,
S4b). No shelf progradation is evident north of Norske Trough within MU-1, possibly indicating that the ice sheet
495  did not reach the palaeo-shelf edge at the IT-A bank.

### 5.1.2  Stage 2 - Late Miocene ice sheet expansion (6.4 – 4.1 Ma)

The lateral distribution of MU-2 is much greater than MU-1, with depocentres located outside both Norske Trough
(and surrounding areas) and Westwind Trough that are interpreted as TMFs. MU-2 is thus interpreted to represent
500  a north and eastward expansion of the former GrIS, occurring between the late Miocene to early Pliocene (6.4 –
4.1 Ma) (Figs. 7b, 8). The time interval which MU-2 spans corresponds to a peak in IRD occurrences in the Fram
Strait around 6 Ma and a gradual decrease towards the end of the period interrupted by several IRD peaks (Fig. 8).

Outside Westwind Trough and northern IT-A bank, the thickness map of MU-2 shows two barely connected
depocentres, possibly indicating two ice streams operating in this area during the deposition of this unit: one
505  draining through the Westwind Trough, and another draining ice from the northern IT-A bank (Fig. 7b). The
suggested ice streams contributed to minimal shelf progradation, perhaps due to the steeply inclined palaeo-surface
off Westwind Trough and northern IT-A bank (Figs. 6a, 6c). The largest depocentre of MU-2 stretches across the
entire width of Norske and Store Koldewey Trough and onto the adjacent bank areas. The thickest part of this
depocentre indicates that the most intense ice streaming, and sediment deposition, was located on the southern part
510  of Norske Trough, between the two depocentres of MU-1 (Figs. 7a-b), therefore indicating a slight switching of
ice streaming position between deposition of MU-1 and MU-2. The broadening of the depocentre on the southern
IT-A bank, seismically characterized by prograded fill sourced from the NW (Figs. 4a-b), indicates ice streams
draining from the IT-A bank towards the SE, depositing sediments in the accommodation space north of Norske
Trough. The ice stream operating in Store Koldewey Trough and IT-C bank during deposition of MU-1 seems to
515  have been slightly reduced or reorganized during deposition of MU-2 (Figs. 7a-b). The low sediment thickness on
the central outer IT-A bank may indicate that the ice sheet did not reach the shelf edge at this location or that ice
reaching the shelf edge was cold based, with little sediment transportation towards the shelf edge during this period.

Altogether, MU-2 tells a story of a laterally expanding GrIS towards the north and east that now covered large
parts of the shelf, with active ice streaming in the two northernmost troughs and on the banks. Whether the ice
520  streams on the IT-A bank were sourced by a local ice dome on the inner, shallowest part of the shelf or by
overflowing ice from the continental GrIS is unknown. Arndt et al. (2015) speculated that such an ice dome could
have been supported by low sea level stands during glaciations. We do not know whether the ice streams we
propose on the IT-A bank were active simultaneously. However, our findings show that dynamic grounded ice
was established both in the troughs and on the IT-A bank already during the late Miocene and continued into the
525  early Pliocene.

### 5.1.3   Stage 3 - Major change in ice sheet configuration (4.1 – 0 Ma)

Following the deposition of MU-2 we see a change in the depositional pattern on the outer shelf and slope marked by a Pliocene unconformity, NEG-3 (4.1±0.3 Ma). MU-3 is comprised of thick, coherent sedimentary deposits, representing intense shelf progradation and deposition of multiple TMFs from after 4.1 Ma to recent time (Figs. 6h, 7c). The shelf trajectory off Norske Trough slightly differs from the previous MU-1 and MU-2, creating the unconformity seen on the seismic data (Figs. 3, 4c-d). It is also possible that NEG-3 represents a depositional hiatus or low sedimentation rates of an unknown duration. The coherency of the seismic unit suggests that the GrIS extended across the entire shelf and to the shelf edge, probably multiple times during deposition of MU-3. The boundary between MU-2 and MU-3 corresponds to a small IRD peak in the Fram Strait at around 4.1 Ma (Fig. 8). This event may coincide with the first glacial episode recorded in MU-3 or the last advance/deglaciation recorded in MU-2. The IRD flux through the Fram Strait between 3.9 – 3.4 Ma is uncertain due to low recovery from the ODP Site 909 at this interval, but the IRD flux is again reported to increase from c. 3.3 Ma, with the first major peak at the Plio-Pleistocene boundary and high IRD flux throughout most of Pleistocene (Fig. 8c).

The thickest parts of MU-3 indicate the locations that have been dominated by ice streams during deposition, with the most intense ice streaming occurring across the whole width of the present-day Norske Trough and Westwind Trough (Figs. 6, 7c). In contrast to MU-2, the MU-3 depocentre outside Westwind Trough forms a single continuously thick deposit that stretches the whole width of Westwind Trough and parts of the northern IT-A bank. This may indicate that ice streams operating in both Westwind Trough and on the IT-A bank during this period terminated in close proximity to each other or alternatively, if they operated contemporaneously, merged close to the shelf edge forming a single TMF. A shallower area on both the present day and palaeo-seafloor central on the northern IT-A bank may have acted as a barrier, dividing the two ice streams operating in Westwind Trough and on IT-A bank further in on the shelf (Fig. 7c). However, based on our current dataset we cannot distinguish whether this TMF was deposited during synchronous ice streaming in both areas and if they were active during different time periods.

The operation of ice streams on the bank is confirmed by the depocentre located central on outer IT-A bank. This depocentre indicates that ice streams have drained eastwards from central IT-A bank, turning slightly towards the NE close to its terminus at the shelf edge, where it formed a TMF, seen as a bulge in the present-day shelf at this location (Figs. 6d, 6h, 7c). The depocentre on outer Norske Trough and southern IT-A bank is testament to widespread and probably reoccurring ice streaming within the trough, through many glacial cycles, forming a massive and coherent TMF.

Interestingly, at this scale, Store Koldewey Trough does not stand out with its own separate depocentre within MU-3, instead, the elongated depocentre from Norske Trough stretches south and covers most of the outer Store Koldewey Trough (Fig. 7b). Thus, any deposits originating from an ice stream operating in Store Koldewey Trough may have extended the depocentre of Norske Trough towards the south. Additionally, this may indicate that the role of the contemporary Store Koldewey Trough as an ice stream conduit during the late Pliocene and the whole of Pleistocene was relatively small. A possible explanation for this is that the Store Koldewey Trough as seen today formed relatively recently, possibly during the last few glaciations. This is supported by our observations that the main sediment delivery, and therefore ice streaming, across the shelf in this area actually

565    seems to have occurred across the IT-C bank (MU-1 and MU-2), just south of Store Koldewey Trough, and not
within the present-day trough itself (Figs. 7a-c).

The southernmost depocentre mapped in this study is located on the upper slope off IT-C bank. The full size and
lateral distribution of this depocentre is not clear as this area suffers from poor data coverage, in addition to strong
seafloor multiples on the shelf, making the lateral correlation of shallow reflections uncertain. However, our results

570    suggest that the main sediment contribution came from the IT-C bank, or possibly further south. The shelf deposits
on IT-C are dominated by aggrading semi-horizontal strata, possibly indicating that the ice streaming across IT-C
bank had ceased by deposition of MU-3.
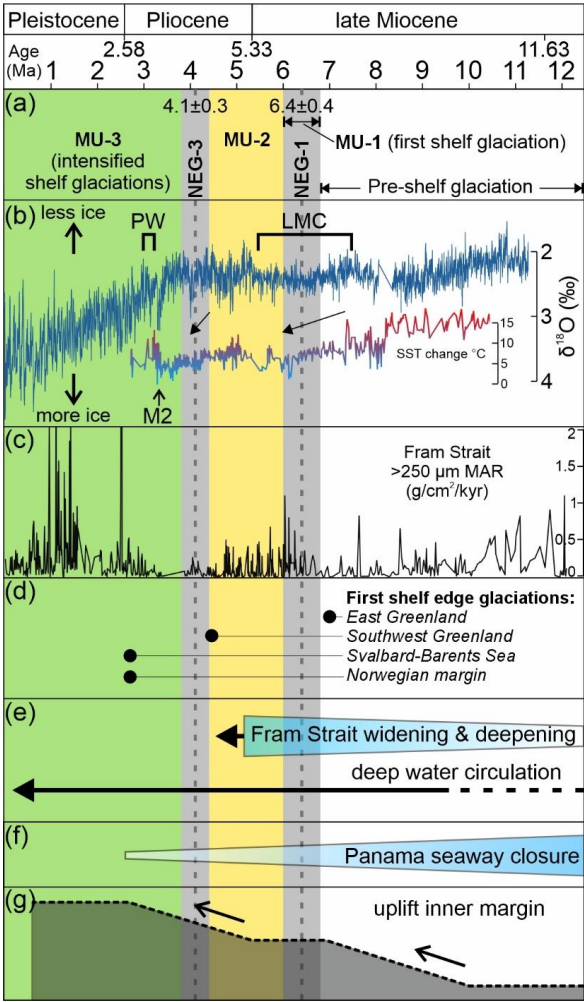
**Figure 8: Chronological correlation of climatic, glacial and tectonic events to the major stratigraphical changes we
575    describe in this study. a) Seismic mega units (MU) mapped in this study with their respective bounding horizons
(dashed line) and estimated error margin (gray background). b) PW: mid-Pliocene warmth (c. 3.3 – 3.0 Ma). LMC:
late Miocene cooling (c. 7.5 – 5.5 Ma). M2: Marine isotope stage M2 (c. 3.3 Ma). Pacific benthic foraminiferal δ18O
spanning 0 – 11.5 Ma modified from Miller et al. (2020). SST change: sea surface temperature changes from the
Norwegian Sea spanning 10.5 – 2.86 Ma modified from Herbert et al. (2016). Arrows highlights trends of δ18O and**

580    **SST at the intervals corresponding to our key reflections. c) IRD mass accumulation rates (MAR) from ODP site 909 in the Fram Strait modified from Gruetzner et al. (2022). d) Black circles mark the oldest known records of shelf edge glaciations off Blosseville Kyst, East Greenland at c. 7 Ma (Pérez et al., 2018), Southwest Greenland at c. 4.6 Ma (Nielsen & Kuijpers, 2013), Svalbard-Barents Sea (Knies et al., 2009) and Norwegian margin at 2.7 Ma (Eidvin et al., 1993). e) Oceanographic setting in the Fram Strait, eventually allowing deep water circulation after around 9.8 Ma**

585    **(Kristoffersen, 1990; Engen et al., 2008). f) Closure of the Panama Seaway 13 – 2.6 Ma (Lunt et al., 2008). g) late Miocene and early Pliocene tectonic uplift of the inner NE Greenland margin (Døssing et al., 2016; Bonow and Japsen, 2021).**

### 5.2    Greenland ice sheet history in a global context

590    #### 5.2.1    Late Miocene (11.63 – 5.33 Ma)

Deep-marine sedimentary records of sporadic IRDs from the Norwegian-Greenland Sea indicate ephemeral glacial ice in Greenland already during Eocene and Oligocene times (Eldrett et al., 2007; Tripati et al., 2008). After 12 – 11 Ma, sediment records from this region indicates more or less continuous IRD in the deep marine environment (Fig. 8c) (Fronval & Jansen, 1996; Thiede, 2011; Gruetzner et al., 2022). This suggests that parts of the benthic

595    $\delta^{18}O$ enrichments and sea level falls following this period (Fig. 8b) (Miller et al., 2020) can be attributed to late Miocene Northern Hemisphere ice sheet growth, a time when global sea surface temperatures were declining (Herbert et al., 2016). Lithological analysis of the IRD has suggested Greenland as the main source area for northern North Atlantic IRD (Bierman et al., 2016), but also Svalbard and the northern Barents Sea contributed with ice rafting through the Fram Strait from around 11 Ma (Knies & Gaina, 2008; Gruetzner et al., 2022). This

600    indicates ice sheet growth or local coastal glaciers on both sides of the Fram Strait large enough to reach sea level.

Seismostratigraphic studies on the SE and eastern Greenland margin have shown that massive shelf progradation initiated around 7 Ma (Larsen et al., 1994; Pérez et al., 2018), simultaneously with increased accumulation of IRD in the adjacent deep ocean basins (St John & Krissek, 2002). These records provide indirect evidence of an ice sheet or coastal glaciers terminating at sea level, but no further constraints on ice sheet extent. As a result of these

605    observations, SE Greenland was initially suggested as a nucleation site for the early growth of the GrIS and marine terminating coastal glaciers (Larsen et al., 1994; St John & Krissek, 2002), causing higher sedimentation rates on the shelf and iceberg production carrying IRDs towards the deep ocean basins. This timing closely aligns with our suggested onset of shelf glaciation on NE Greenland at 6.4±0.4 Ma. Thus, our findings add new and rare information on the extent and dynamics of the late Miocene GrIS and confirm late Miocene ice sheet growth did

610    not only occur in SE and central eastern Greenland as previously proposed, but also in NE Greenland. This has implications for modelling of the late Miocene GrIS ice budget and its effect on the global sea level budget which has not yet been constrained for this period and is probably much higher than anticipated (Miller et al., 2020). Furthermore, based on the currently available research discussed here and our new observations from NE Greenland, we may hypothesise that the entire eastern margin led the onset of shelf glaciation on Greenland by

615    about 2 million years and led the rest of the Northern Hemisphere by almost 4 million years prior to the Plio-Pleistocene intensification at 2.7 Ma.

#### 5.2.2    Pliocene (5.33 – 2.58 Ma)

The Miocene-Pliocene transition is generally characterized by decreasing benthic $\delta^{18}O$ values and rising sea levels,

620    indicating warmer climate and reduced global ice volume in the Pliocene, accompanied by higher $pCO_2$

concentrations in the atmosphere (Fig. 8b) (Miller et al., 2020). However, despite the relative early Pliocene warmth, the presence of a GrIS is evident by continuous records of IRDs in the northern North Atlantic and Norwegian-Greenland Sea throughout the Pliocene (Fronval & Jansen, 1996; Bierman et al., 2016; Gruetzner et al., 2022). Moreover, debris flow deposits from a marine sediment core off the Scoresby Sund fan were interpreted

625 to indicate glacial advance across the shelf at around 5 Ma (Butt et al., 2001), whilst similar deposits offshore SW Greenland are suggested to mark first glacial advance across this shelf sector around 4.5 Ma (Fig. 8d) (Nielsen & Kuijpers, 2013). Consistent with our results, these observations support the notion that the GrIS reached the shelf across NE, E and SW Greenland during the early Pliocene, corresponding to our seismic mega unit MU-2 (Fig. 8).

630 De Schepper et al. (2014) synthesized terrestrial and marine evidence of Pliocene glaciations in the Northern and Southern Hemisphere and concluded that four major glacial expansions occurred globally around 4.9 – 4.8, 4.0, 3.6 and 3.3 Ma, falling within the timeframe of our seismic units MU-2 and MU-3 (Fig. 8). At 4.9 – 4.8 Ma the Greenland and Scandinavian Ice Sheets were main contributors to northern North Atlantic IRD, with additional inputs from North America and the Svalbard-Barents Sea region by 4.0 Ma (De Schepper et al., 2014) indicating

635 conditions that increasingly favour ice sheet growth in the Northern Hemisphere, despite the relatively warm Pliocene climate. This is consistent with our findings that indicate multiple advances of the GrIS across the NE Greenland shelf through the Pliocene and a change in the ice sheet configuration and intensification of ice streaming across the shelf, here suggested after 4.1 Ma. However, the Pliocene unconformity (NEG-3) identified in this study only provide a maximum age of MU-3, thus the exact timing of intensification across the shelf is not

640 fully known, as we cannot rule out that NEG-3 marks a hiatus or a period of low sedimentation rates.

From 3.6 Ma and onwards, the global ice volume increased, culminating at c. 3.3 Ma during marine isotope stage (MIS) M2, recognized as the first major marine isotope enrichment during late Pliocene (Fig. 8b) (Lisiecki & Raymo, 2005; De Schepper et al., 2014; Miller et al., 2020), corresponding to low sea surface temperatures in the Norwegian Sea (Herbert et al., 2016). This period marks a transitional phase before the onset of the intensification

645 of the Northern Hemisphere glaciations (iNHG) at 2.7 Ma (De Schepper et al., 2014). Thus, the true onset of MU-3 may be of late Pliocene age  (3.6 – 2.7 Ma), coinciding with the onset of the iNHG and the initiation of shelf glaciations on e.g. the Svalbard-Barents Sea (Knies et al., 2009; Mattingsdal et al., 2014) and Norwegian margin (Fig. 8d) (Eidvin et al., 1993; Ottesen et al., 2009). Remnants of spruce and thuja and relatively temperate marine biomarkers of late Pliocene age are described from raised marine sediments on Île de France, an island located in

650 NE Greenland (Bennike et al., 2002). These indicate periodically higher-than-present air temperatures and an ice-free coastline during late Pliocene, corroborating that MU-3 was not deposited by continuous shelf glaciations since 4.1 Ma, but rather episodic and intense advances of the GrIS after. This is consistent with the stratigraphy of the Kap København Formation in Northern Greenland, where shallow marine successions are situated between till beds, indicating warmer interglacial periods in late Pliocene and Early Pleistocene (Funder et al., 2001).

655

### 5.3 External forcings on Greenland Ice Sheet growth

The response of ice sheets to external forcings is extremely complex, but key to understand past and future scenarios to a changing climate. The warmer climate during the Pliocene seems contradictory to ice sheet growth in general and to shelf-wide, marine terminating ice sheets especially. Yet, persistent circum-arctic glaciers

660    reaching the coast through much of late Miocene and the whole of Pliocene is indicated by consistent IRD records
        in northern North Atlantic marine sediment cores (Knies & Gaina, 2008; Bierman et al., 2016; Gruetzner et al.,
        2022). This study has for the first time shown detailed evidence of glacial ice extended across the NE Greenland
        continental shelf since late Miocene. Following is an overview of key external forcings that possibly facilitated
        ice sheet growth in Greenland during late Miocene and Pliocene (Fig. 8).

665    Oceanographic factors play a key role in regulating regional temperatures and precipitation, potentially affecting
        regional and global ice budgets, thus the Fram Strait is a key oceanic gateway with respect to the NE Greenland
        and Svalbard margins (Fig. 1). Although the opening of the Fram Strait commenced already in the earliest
        Oligocene (Engen et al., 2008), deep water exchange was not established until early-middle Miocene (20 – 15 Ma)
        (Jakobsson et al., 2007) or possibly late Miocene (9.8 Ma) (Engen et al., 2008), when it became wide and deep
670    enough to allow deep water circulation (Fig. 8e). The closure of the Panama seaway ~13 – 2.6 Ma led to
        strengthening of the Atlantic thermohaline circulation and increased temperatures and precipitation in the Northern
        Hemisphere (Fig. 8f) (Lunt et al., 2008). The middle and late Miocene was a time of general global cooling in the
        wake of the Miocene Climatic Optimum (c. 17 – 15 Ma; MCO). Reconstructions of global alkenone sea surface
        temperatures (SST) during the last 12 million years have shown that the SST cooling at mid to high-latitudes
675    accelerated synchronous in both hemispheres in the latest Miocene (c. 7.5 – 5.5 Ma) (Herbert et al., 2016). During
        that period, the SSTs decreased about 8°C and were close to present-day temperatures (Fig. 8b), possibly driven
        by declining atmospheric $CO_2$ (Herbert et al., 2016). This period, referred to as the late Miocene cooling (LMC),
        coincides with the onset of early shelf glaciations represented by MU-1 and possibly parts of MU-2 in this study.
        Knies and Gaina (2008) argued that the opening of the Fram Strait resulted in increased precipitation, coupled with
680    general global cooling in the late Miocene facilitated ice sheet growth in the northern Barents Sea and Svalbard at
        the time, and a similar coupling is likely for our study area. Enhanced snowfall driven by sea ice loss during warm
        periods has recently been suggested as a mechanism to promote ice sheet growth and advance in Arctic settings
        (Auer et al., 2025), and a similar feedback mechanism may have played a crucial role during the Late Miocene
        and Pliocene in NE Greenland.

685    Moreover, circum-Arctic tectonic uplift has been proposed as a controlling factor for ice sheet growth and stability
        (Solgaard et al., 2013; De Schepper et al., 2014; Japsen et al., 2014; Knies et al., 2014). Indeed, Greenland
        experienced two kilometre-scale Neogene uplift events during the late Miocene (~10 Ma), and early Pliocene (~5
        Ma) (Japsen et al., 2006; Japsen et al., 2014; Bonow & Japsen, 2021). Both events led to significant uplift of the
        eastern and NE Greenland inner margin (Fig. 8g) (Døssing et al., 2016; Bonow & Japsen, 2021). Solgaard et al.
690    (2013) modelled the effect of Neogene tectonic uplift on ice sheet growth on Greenland, showing that increased
        precipitation together with decreased temperatures following higher elevation strongly promoted continental ice
        sheet growth along most of east Greenland. With present-day sea surface temperatures as input, the modelled GrIS
        quickly grew to cover large parts of the northern and eastern Greenland after the first late Miocene uplifting event
        but struggled to cover the central and western parts of Greenland due to Föhn effect and a precipitation shadow in
695    central and western Greenland. Subsequently, the model predicted that a GrIS could cover the whole of Greenland
        following the second uplift event in the early Pliocene. The eastern extent of the modelled ice sheet is limited to
        the coast, but any uplift and potential subaerial exposure of the present-day shelf was not included in the model.

Whether or not parts of the shelf in our study area ever were subaerial exposed is unknown, but not unthinkable, considering the very shallow depths on the inner parts of the IT-A bank (Fig. 1).

700 Considering that most of the modelled available precipitation is located along the east coast, and assuming that the elevated topography limited ice sheet drainage towards west, an eastward expansion of the GrIS across an uplifted shelf seems very likely and is in line with our newly presented observations of late Miocene onset for shelf glaciation on NE Greenland. Thus, we argue that tectonic uplift coupled with changing oceanographic settings after opening of the Fram Strait and general global cooling during the LMC facilitated ice sheet growth along the
705 entire east Greenland margin during late Miocene, culminating in the first advance of the GrIS across the NE Greenland shelf at around 6.4 Ma.

## 6    Conclusions

This study has defined three regional seismic mega units (MU-1, MU-2 & MU-3) on the Northeast Greenland
710 margin, bounded by major unconformable reflections termed NEG-1, NEG-2 and NEG-3. The interpreted unconformable reflection NEG-1 correlates with the Inter-Miocene Unconformity (IMU) interpreted by previous studies in the Greenland Basin. We have extended this horizon to the Molloy Basin and tied it to ODP Site 909 which yield an age of 6.4±0.4 for this horizon.

MU-1 marks the onset of widespread shelf progradation during late Miocene at around 6.4 Ma, driven by the first
715 recorded advance of grounded ice masses (ice streams) to the shelf edge, forming large trough mouth fans on the upper palaeo-slope. The first ice streams to reach the shelf edge were located within Norske Trough and on the IT-C bank and southern part of Store Koldewey Trough, probably constrained by pre-glacial topography. The onset of shelf glaciation coincides with increased flux of ice rafted debris into the northern seas during the late Miocene cooling, uplift of the inner margin, and widening/deepening of the Arctic-Atlantic Gateway through the Fram Strait
720 enabling deep water circulation and northwards transport of moisture.

Our analysis reveal that ice streams continued to cross the shelf in Norske Trough multiple times during the late Miocene and early Pliocene (c. 6.4 – 4.1 Ma), with additional ice streams operating in Westwind Trough and on the IT-A bank, indicating a dynamic Greenland Ice Sheet during this period with increased potential to expand across the shelf, possibly driven by the external forcings mentioned above.

725 A major change in ice sheet configuration post-dates the Pliocene unconformity here dated to 4.1±0.3 Ma. Whereas previous Greenland Ice Sheet expansions may have been more ephemeral and not covered the entire shelf, we now see evidence of a fully developed ice sheet that expands across the entire NE Greenland shelf, with widespread ice streaming documented on the banks and troughs. We hypothesise that the Pliocene unconformity (NEG-3) may represent a depositional hiatus or a condensed section and that the onset of intensified ice streaming across the NE
730 Greenland shelf and deposition of MU-3 coincides with the intensification of the Northern Hemisphere glaciations between ~3.6 to ~2.7 Ma.

**Data availability**

735    Open access seismic data can be requested through the GNPDR portal (www.greenpetrodata.gl), or through the
GEUS data archive. For permission to access the confidential seismic data please contact TGS.

**Author contributions**

FWJ, MW, JSL, APF, ALQ and TN participated in the conceptualization of this study. FWJ carried out the
740    investigation and prepared the manuscript with critical contributions from all co-authors. TN, CB, BB and SP
contributed with data curation. MW, JSL and APF contributed with supervision.

**Competing interests**

The authors declare that they have no conflict of interest.

745

**Acknowledgement**

We are grateful to TGS and GEUS for making seismic data available to this study. Partners at GEUS provided
GXT surveys from 2010 and 2011 and helped to fix navigation issues with the Kanumas surveys. The AWI surveys
used here were reprocessed by TGS in 2010 and, along with TGS surveys from 2013 and 2014. The remaining
750    open access data are available through the GNPDR portal (www.greenpetrodata.gl), or through the GEUS data
archive. For permission to access the seismic data, please contact the institutions mentioned here. Scientific colour
maps courtesy of Crameri et al. (2020).

**Financial support**

755    The work by FWJ, MW and APF forms a part of iC3: Centre for ice, Cryosphere, Carbon and Climate and were
supported by the Research Council of Norway through the Centres of Excellence funding scheme, project number
332635. The work of CB has been funded by the European Union under Horizon Europe grant agreement No
101060851 (GreenFlux). JSL acknowledge support from the Research Council of Norway through the DYPOLE
project (grant no. 325984).

760

Arndt, J. E., Jokat, W., & Dorschel, B. (2017). The last glaciation and deglaciation of the Northeast Greenland
765        continental shelf revealed by hydro-acoustic data. *Quaternary Science Reviews*, *160*, 45-56.
https://doi.org/10.1016/j.quascirev.2017.01.018

Arndt, J. E., Jokat, W., Dorschel, B., Myklebust, R., Dowdeswell, J. A., & Evans, J. (2015). A new bathymetry of the Northeast Greenland continental shelf: Constraints on glacial and other processes. *Geochemistry Geophysics Geosystems*, *16*(10), 3733-3753. https://doi.org/10.1002/2015gc005931

770   Auer, A. G., van der Bilt, W. G. M., Schomacker, A., Bakke, J., Storen, E. W. N., Buckby, J. M., Cederstrom, J. M., & van der Plas, S. (2025). Hydroclimate intensification likely aided glacier survival on Svalbard in the Early Holocene. *Communications Earth & Environment*, *6*(1). https://doi.org/10.1038/s43247-025-02064-z

Batchelor, C. L., & Dowdeswell, J. A. (2014). The physiography of High Arctic cross-shelf troughs. *Quaternary

775   Science Reviews*, *92*, 68-96. https://doi.org/10.1016/j.quascirev.2013.05.025

Bennike, O., Abrahamsen, N., Bak, M., Israelson, C., Konradi, P., Matthiessen, J., & Witkowski, A. (2002). A multi-proxy study of Pliocene sediments from Ile de France, North-East Greenland. *Palaeogeography Palaeoclimatology Palaeoecology*, *186*(1-2), 1-23. https://doi.org/10.1016/S0031-0182(02)00439-X

Berger, D., & Jokat, W. (2008). A seismic study along the East Greenland margin from 72°N to 77°N. *Geophysical

780   Journal International*, *174*(2), 733-748. https://doi.org/10.1111/j.1365-246X.2008.03794.x

Bierman, P. R., Shakun, J. D., Corbett, L. B., Zimmerman, S. R., & Rood, D. H. (2016). A persistent and dynamic East Greenland Ice Sheet over the past 7.5 million years. *Nature*, *540*(7632), 256-+. https://doi.org/10.1038/nature20147

Bonow, J. M., & Japsen, P. (2021). Peneplains and tectonics in North-East Greenland after opening of the

785   North-East Atlantic. *Geus Bulletin*, *45*(1). https://doi.org/10.34194/geusb.v45.5297

Butt, F. A., Elverhoi, A., Forsberg, C. F., & Solheim, A. (2001). Evolution of the Scoresby Sund Fan, central East Greenland - evidence from ODP Site 987. *Norsk Geologisk Tidsskrift*, *81*(1), 3-15. https://njg.geologi.no/images/NJG_articles/NGT_81_1_003-015.pdf

Cooper, A. K., Barrett, P. J., Hinz, K., Traube, V., Leitchenkov, G., & Stagg, H. M. J. (1991). Cenozoic Prograding

790   Sequences of the Antarctic Continental-Margin - a Record of Glacioeustatic and Tectonic Events. *Marine Geology*, *102*(1-4), 175-213. https://doi.org/10.1016/0025-3227(91)90008-R

Crameri, F., Shephard, G. E., & Heron, P. J. (2020). The misuse of colour in science communication. *Nature Communications*, *11*(1). https://doi.org/10.1038/s41467-020-19160-7

Dahlgren, K. I. T., Vorren, T. O., & Laberg, J. S. (2002). Late Quaternary glacial development of the mid-

795   Norwegian margin -: 65 to 68°N. *Marine and Petroleum Geology*, *19*(9), 1089-1113. https://doi.org/10.1016/S0264-8172(03)00004-7

Dahlgren, K. I. T., Vorren, T. O., Stoker, M. S., Nielsen, T., Nygård, A., & Sejrup, H. P. (2005). Late Cenozoic prograding wedges on the NW European continental margin:: their formation and relationship to tectonics and climate. *Marine and Petroleum Geology*, *22*(9-10), 1089-1110.

800   https://doi.org/10.1016/j.marpetgeo.2004.12.008

De Schepper, S., Gibbard, P. L., Salzmann, U., & Ehlers, J. (2014). A global synthesis of the marine and terrestrial evidence for glaciation during the Pliocene Epoch. *Earth-Science Reviews*, *135*, 83-102. https://doi.org/10.1016/j.earscirev.2014.04.003

Dowdeswell, J. A., & Elverhøi, A. (2002). The timing of initiation of fast-flowing ice streams during a glacial cycle

805   inferred from glacimarine sedimentation. *Marine Geology*, *188*(1-2), 3-14. https://doi.org/10.1016/S0025-3227(02)00272-4

Dowdeswell, J. A., Ottesen, D., & Rise, L. (2006). Flow switching and large-scale deposition by ice streams draining former ice sheets. *Geology*, *34*(4), 313-316. https://doi.org/10.1130/G22253.1

Døssing, A., Japsen, P., Watts, A. B., Nielsen, T., Jokat, W., Thybo, H., & Dahl-Jensen, T. (2016). Miocene uplift of

810   the NE Greenland margin linked to plate tectonics: Seismic evidence from the Greenland Fracture Zone, NE Atlantic. *Tectonics*, *35*(2), 257-282. https://doi.org/10.1002/2015tc004079

Eidvin, T., Jansen, E., & Riis, F. (1993). Chronology of Tertiary fan deposits off the western Barents Sea: Implications for the uplift and erosion history of the Barents Shelf. *Marine Geology*, *112*(1-4), 109-131.

Eldrett, J. S., Harding, I. C., Wilson, P. A., Butler, E., & Roberts, A. P. (2007). Continental ice in Greenland during

815   the Eocene and Oligocene. *Nature*, *446*(7132), 176-179. https://doi.org/10.1038/nature05591

Engen, O., Faleide, J. I., & Dyreng, T. K. (2008). Opening of the Fram Strait gateway: A review of plate tectonic constraints. *Tectonophysics*, *450*(1-4), 51-69. https://doi.org/10.1016/j.tecto.2008.01.002

Fronval, T., & Jansen, E. (1996). Late Neogene pateoclimates and paleoceanography in the Iceland-Norwegian Sea: evidence from the Iceland and Vøring Plateaus. PROCEEDINGS-OCEAN DRILLING PROGRAM

820   SCIENTIFIC RESULTS,

Funder, S., Bennike, O., Böcher, J., Israelson, C., Petersen, K. S., & Símonarson, L. A. (2001). Late Pliocene Greenland -: The Kap Kobenhavn Formation in North Greenland. *Bulletin of the Geological Society of Denmark*, *48*, 117-134.

Funder, S., Kjeldsen, K. K., Kjær, K. H., & Cofaigh, C. Ó. (2011). The Greenland Ice Sheet during the past 300,000
825        years: A review. *Developments in Quaternary Sciences*, *15*, 699-713. https://doi.org/10.1016/B978-0-
444-53447-7.00050-7

Fyhn, M. B. W., Hopper, J. R., Sandrin, A., Lauridsen, B. W., Heincke, B. H., Nohr-Hansen, H., Andersen, M. S.,
Alsen, P., & Nielsen, T. (2021). Three-phased latest Jurassic-Eocene rifting and mild mid-Cenozoic
compression offshore NE Greenland. *Tectonophysics*, *815*.
830        https://doi.org/10.1016/j.tecto.2021.228990

Gruetzner, J., Matthiessen, J., Geissler, W. H., Gebhardt, A. C., & Schreck, M. (2022). A revised core-seismic
integration in the Molloy Basin (ODP Site 909): Implications for the history of ice rafting and ocean
circulation in the Atlantic-Arctic gateway. *Global and Planetary Change*, *215*.
https://doi.org/10.1016/j.gloplacha.2022.103876

835 Hamann, N. E., Whittaker, R. C., & Stemmerik, L. (2005). Geological development of the Northeast Greenland
Shelf. In A. G. Doré & B. A. Vining (Eds.), *Petroleum Geology: North-West Europe and Global
Perspectives—Proceedings of the 6th Petroleum Geology Conference* (Vol. 6, pp. 0). Geological Society
of London. https://doi.org/10.1144/0060887

Helland, P. E., & Holmes, M. A. (1997). Surface textural analysis of quartz sand grains from ODP Site 918 off the
840        southeast coast of Greenland suggests glaciation of southern Greenland at 11 Ma. *Palaeogeography
Palaeoclimatology Palaeoecology*, *135*(1-4), 109-121. https://doi.org/10.1016/S0031-0182(97)00025-4

Herbert, T. D., Lawrence, K. T., Tzanova, A., Peterson, L. C., Caballero-Gill, R., & Kelly, C. S. (2016). Late Miocene
global cooling and the rise of modern ecosystems. *Nature Geoscience*, *9*(11), 843-+.
https://doi.org/10.1038/Ngeo2813

845 Hull, D. M., Osterman, L. E., & Thiede, J. (1996). *35. BIOSTRATIGRAPHIC SYNTHESIS OF LEG 151, NORTH
ATLANTIC-ARCTIC GATEWAYS* (Proceedings of the Ocean Drilling program, Scientific Results, Issue.

Hvidberg, C. S., Grinsted, A., Dahl-Jensen, D., Khan, S. A., Kusk, A., Andersen, J. K., Neckel, N., Solgaard, A.,
Karlsson, N. B., Kjær, H. A., & Vallelonga, P. (2020). Surface velocity of the Northeast Greenland Ice
Stream (NEGIS): assessment of interior velocities derived from satellite data by GPS. *Cryosphere*,
850        *14*(10), 3487-3502. https://doi.org/10.5194/tc-14-3487-2020

Jakobsson, M., Backman, J., Rudels, B., Nycander, J., Frank, M., Mayer, L., Jokat, W., Sangiorgi, F., O'Regan, M.,
Brinkhuis, H., King, J., & Moran, K. (2007). The early Miocene onset of a ventilated circulation regime
in the Arctic Ocean. *Nature*, *447*(7147), 986-990. https://doi.org/10.1038/nature05924

Jakobsson, M., Mohammad, R., Karlsson, M., Salas-Romero, S., Vacek, F., Heinze, F., Bringensparr, C., Castro, C.
855        F., Johnson, P., Kinney, J., Cardigos, S., Bogonko, M., Accettella, D., Amblas, D., An, L., Bohan, A.,
Brandt, A., Buenz, S., Canals, M.,…Mayer, L. (2024). The International Bathymetric Chart of the Arctic
Ocean Version 5.0. *Scientific Data*, *11*(1). https://doi.org/10.1038/s41597-024-04278-w

Japsen, P., Bonow, J. M., Green, P. F., Chalmers, J. A., & Lidmar-Bergström, K. (2006). Elevated, passive
continental margins: Long-term highs or neogene uplifts? New evidence from West Greenland. *Earth
860        and Planetary Science Letters*, *248*(1-2), 330-339. https://doi.org/10.1016/j.epsl.2006.05.036

Japsen, P., Green, P. F., Bonow, J. M., Nielsen, T. F. D., & Chalmers, J. A. (2014). From volcanic plains to
glaciated peaks: Burial, uplift and exhumation history of southern East Greenland after opening of the
NE Atlantic. *Global and Planetary Change*, *116*, 91-114.
https://doi.org/10.1016/j.gloplacha.2014.01.012

865 Knies, J., & Gaina, C. (2008). Middle miocene ice sheet expansion in the Arctic: Views from the Barents Sea.
*Geochemistry Geophysics Geosystems*, *9*. https://doi.org/10.1029/2007GC001824

Knies, J., Matthiessen, J., Vogt, C., Laberg, J. S., Hjelstuen, B. O., Smelror, M., Larsen, E., Andreassen, K., Eidvin,
T., & Vorren, T. O. (2009). The Plio-Pleistocene glaciation of the Barents Sea-Svalbard region: a new
model based on revised chronostratigraphy. *Quaternary Science Reviews*, *28*(9-10), 812-829.
870        https://doi.org/10.1016/j.quascirev.2008.12.002

Knies, J., Mattingsdal, R., Fabian, K., Grosfjeld, K., Baranwal, S., Husum, K., De Schepper, S., Vogt, C., Andersen,
N., Matthiessen, J., Andreassen, K., Jokat, W., Nam, S. I., & Gaina, C. (2014). Effect of early Pliocene
uplift on late Pliocene cooling in the Arctic-Atlantic gateway. *Earth and Planetary Science Letters*, *387*,
132-144. https://doi.org/10.1016/j.epsl.2013.11.007

875 Knutz, P. C., Newton, A. M. W., Hopper, J. R., Huuse, M., Gregersen, U., Sheldon, E., & Dybkjær, K. (2019).
Eleven phases of Greenland Ice Sheet shelf-edge advance over the past 2.7 million years. *Nature
Geoscience*, *12*(5), 361-+. https://doi.org/10.1038/s41561-019-0340-8

Kristoffersen, Y. (1990). On the tectonic evolution and paleoceanographic significance of the Fram Strait
gateway. In *Geological history of the polar oceans: Arctic versus Antarctic* (pp. 63-76). Springer.
880        https://doi.org/10.1007/978-94-009-2029-3_4

Laberg, J. S., Forwick, M., & Husum, K. (2017). New geophysical evidence for a revised maximum position of part of the NE sector of the Greenland ice sheet during the last glacial maximum. *arktos*, *3*, 1-9. https://doi.org/10.1007/s41063-017-0029-4

885 Laberg, J. S., & Vorren, T. O. (1995). Late Weichselian Submarine Debris Flow Deposits on the Bear-Island-Trough-Mouth-Fan. *Marine Geology*, *127*(1-4), 45-72. https://doi.org/10.1016/0025-3227(95)00055-4

Laberg, J. S., & Vorren, T. O. (1996). The Middle and Late Pleistocene evolution of the Bear Island Trough Mouth Fan. *Global and Planetary Change*, *12*(1-4), 309-330. https://doi.org/10.1016/0921-8181(95)00026-7

Larsen, H. C., Saunders, A. D., Clift, P. D., Beget, J., Wei, W., Spezzaferri, S., Ali, J., Cambray, H., Demant, A., 890 Fitton, G., Fram, M. S., Fukuma, K., Gieskes, J., Holmes, M. A., Hunt, J., Lacasse, C., Larsen, L. M., Lykkeanderson, H., Meltser, A.,…Cliff, P. D. (1994). 7-Million Years of Glaciation in Greenland. *Science*, *264*(5161), 952-955. https://doi.org/10.1126/science.264.5161.952

Lisiecki, L. E., & Raymo, M. E. (2005). A Pliocene-Pleistocene stack of 57 globally distributed benthic δ18O records. *Paleoceanography*, *20*(1). https://doi.org/10.1029/2004pa001071

895 López-Quirós, A., Junna, T., Davies, J., Andresen, K. J., Nielsen, T., Haghipour, N., Wacker, L., Alstrup, A. K. O., Munk, O. L., Rasmussen, T. L., Pearce, C., & Seidenkrantz, M. S. (2024). Retreat patterns and dynamics of the former Norske Trough ice stream (NE Greenland): An integrated geomorphological and sedimentological approach. *Quaternary Science Reviews*, *325*. https://doi.org/10.1016/j.quascirev.2023.108477

900 Lundin, E. (2013, October 15-18). *NE Greenland Stratigraphic Coring Project 2008. Abstract* 3P Arctic, Polar Petroleum Potential Conference & Exhibition, Stavanger, Norway. https://www.searchanddiscovery.com/abstracts/html/2013/90177arctic/abstracts/lund.htm

Lunt, D. J., Valdes, P. J., Haywood, A., & Rutt, I. C. (2008). Closure of the Panama Seaway during the Pliocene: implications for climate and Northern Hemisphere glaciation. *Climate Dynamics*, *30*(1), 1-18. 905 https://doi.org/10.1007/s00382-007-0265-6

Mattingsdal, R., Knies, J., Andreassen, K., Fabian, K., Husum, K., Grosfjeld, K., & De Schepper, S. (2014). A new 6 Myr stratigraphic framework for the Atlantic-Arctic Gateway. *Quaternary Science Reviews*, *92*, 170-178. https://doi.org/10.1016/j.quascirev.2013.08.022

Miller, K. G., Browning, J. V., Schmelz, W. J., Kopp, R. E., Mountain, G. S., & Wright, J. D. (2020). Cenozoic sea-910 level and cryospheric evolution from deep-sea geochemical and continental margin records. *Science Advances*, *6*(20). https://doi.org/10.1126/sciadv.aaz1346

Mitchum, R. M., Vail, P. R., & Sangree, J. B. (1977). Seismic stratigraphy and global changes of sea level: Part 6. Stratigraphic interpretation of seismic reflection patterns in depositional sequences: Section 2. Application of seismic reflection configuration to stratigraphic interpretation.

915 Morlighem, M., & et al. (2022). *IceBridge BedMachine Greenland, Version 5* (NASA National Snow and Ice Data Center Distributed Active Archive Center. https://doi.org/10.5067/GMEVBWFLWA7X

Myhre, A., Thiede, J., & Firth, J. (1995). Proceedings Ocean Drilling Program initial reports. 151: 1-926, College Station, TX (Ocean Drilling Program).

Nagler, T., Rott, H., Hetzenecker, M., Wuite, J., & Potin, P. (2015). The Sentinel-1 Mission: New Opportunities 920 for Ice Sheet Observations. *Remote Sensing*, *7*(7), 9371-9389. https://doi.org/10.3390/rs70709371

Nielsen, T., De Santis, L., Dahgren, K. I. T., Kuijpers, A., Laberg, J. S., Nygård, A., Praeg, D., & Stoker, M. S. (2005). A comparison of the NW European glaciated margin with other glaciated margins. *Marine and Petroleum Geology*, *22*(9-10), 1149-1183. https://doi.org/10.1016/j.marpetgeo.2004.12.007

Nielsen, T., & Kuijpers, A. (2013). Only 5 southern Greenland shelf edge glaciations since the early Pliocene. 925 *Scientific Reports*, *3*. https://doi.org/10.1038/srep01875

Nygård, A., Sejrup, H. P., Haflidason, H., & Bryn, P. (2005). The glacial North Sea Fan, southern Norwegian Margin:: architecture and evolution from the upper continental slope to the deep-sea basin. *Marine and Petroleum Geology*, *22*(1-2), 71-84. https://doi.org/10.1016/j.marpetgeo.2004.12.001

Ó Cofaigh, C., Lloyd, J. M., Callard, S. L., Gebhardt, C., Streuff, K. T., Dorschel, B., Smith, J. A., Lane, T. P., 930 Jamieson, S. S., & Kanzow, T. (2025). Shelf-edge glaciation offshore of northeast Greenland during the last glacial maximum and timing of initial ice-sheet retreat. *Quaternary Science Reviews*, *359*, 109326. https://doi.org/10.1016/j.quascirev.2025.109326

Olsen, I. L., Rydningen, T. A., Forwick, M., Laberg, J. S., & Husum, K. (2020). Last glacial ice sheet dynamics offshore NE Greenland - a case study from Store Koldewey Trough. *Cryosphere*, *14*(12), 4475-4494. 935 https://doi.org/10.5194/tc-14-4475-2020

Ottesen, D., Rise, L., Andersen, E. S., Bugge, T., & Eidvin, T. (2009). Geological evolution of the Norwegian continental shelf between 61°N and 68°N during the last 3 million years. *Norwegian Journal of Geology*, *89*(4), 251-265.

940     Pérez, L. F., Nielsen, T., Knutz, P. C., Kuijpers, A., & Damm, V. (2018). Large-scale evolution of the central-east Greenland margin: New insights to the North Atlantic glaciation history. *Global and Planetary Change*, *163*, 141-157. https://doi.org/10.1016/j.gloplacha.2017.12.010

Peron-Pinvidic, G., & Osmundsen, P. T. (2018). The Mid Norwegian - NE Greenland conjugate margins: Rifting evolution, margin segmentation, and breakup. *Marine and Petroleum Geology*, *98*, 162-184. https://doi.org/10.1016/j.marpetgeo.2018.08.011

945     Petersen, T. G. (2021). New sequence stratigraphic framework on a 'passive' margin: implications for the post-break-up depositional environment and onset of glaciomarine conditions in NE Greenland. *Journal of the Geological Society*, *178*(2). https://doi.org/10.1144/jgs2020-128

Piepjohn, K., von Gosen, W., & Tessensohn, F. (2016). The Eurekan deformation in the Arctic: an outline. *Journal of the Geological Society*, *173*(6), 1007-1024. https://doi.org/10.1144/jgs2016-081

950     Rasmussen, T. L., Pearce, C., Andresen, K. J., Nielsen, T., & Seidenkrantz, M. S. (2022). Northeast Greenland: ice-free shelf edge at 79.4°N around the Last Glacial Maximum 25.5-17.5 ka. *Boreas*, *51*(4), 759-775. https://doi.org/10.1111/bor.12593

Shepherd, A., Ivins, E., Rignot, E., Smith, B., van den Broeke, M., Velicogna, I., Whitehouse, P., Briggs, K., Joughin, I., Krinner, G., Nowicki, S., Payne, T., Scambos, T., Schlegel, N., A, G., Agosta, C., Ahlstrom, A.,

955     Babonis, G., Barletta, V. R.,…Team, I. (2020). Mass balance of the Greenland Ice Sheet from 1992 to 2018. *Nature*, *579*(7798), 233-+. https://doi.org/10.1038/s41586-019-1855-2

Solgaard, A. M., Bonow, J. M., Langen, P. L., Japsen, P., & Hvidberg, C. S. (2013). Mountain building and the initiation of the Greenland Ice Sheet. *Palaeogeography Palaeoclimatology Palaeoecology*, *392*, 161-176. https://doi.org/10.1016/j.palaeo.2013.09.019

960     St John, K. E. K., & Krissek, L. A. (2002). The late Miocene to Pleistocene ice-rafting history of southeast Greenland. *Boreas*, *31*(1), 28-35. https://doi.org/10.1111/j.1502-3885.2002.tb01053.x

StatoilHydro. (2008). *NE Greenland Coring Project 2008 - Summary Report*.

Thiede, J., Jessen, C., Knutz, P., Kuijpers, A., Mikkelsen, N., Nørgaard-Pedersen, N., & Spielhagen, R. F. . (2011). Millions of years of Greenland Ice Sheet history recorded in ocean sediments. *Polarforschung*, *80*(3),

965     141-159.

Tripati, A. K., Eagle, R. A., Morton, A., Dowdeswell, J. A., Atkinson, K. L., Bahe, Y., Dawber, C. F., Khadun, E., Shaw, R. M. H., Shorttle, O., & Thanabalasundaram, L. (2008). Evidence for glaciation in the Northern Hemisphere back to 44 Ma from ice-rafted debris in the Greenland Sea. *Earth and Planetary Science Letters*, *265*(1-2), 112-122. https://doi.org/10.1016/j.epsl.2007.09.045

970     Vorren, T. O., & Laberg, J. S. (1997). Trough mouth fans - Palaeoclimate and ice-sheet monitors. *Quaternary Science Reviews*, *16*(8), 865-881. https://doi.org/10.1016/S0277-3791(97)00003-6

Winkler, A., Wolf-Welling, T. C. W., Stattegger, K., & Thiede, J. (2002). Clay mineral sedimentation in high northern latitude deep-sea basins since the Middle Miocene (ODP Leg 151, NAAG). *International Journal of Earth Sciences*, *91*(1), 133-148. https://doi.org/10.1007/s005310100199

975